UNIVERSITÀ DEGLI STUDI DI MILANO

Dottorato di ricerca in Scienze Morfologiche XXVII ciclo

THREE-DIMENSIONAL ANALYSIS OF PALATE MORPHOLOGY IN UNILATERAL CLEFT LIP AND PALATE CHILDREN

Coordinatore: Prof. Virgilio F. Ferrario

Tutore: Prof.ssa Chiarella Sforza

Tesi di Dottorato di

LUCA PISONI

Matr. N° R09730

Anno Accademico 2013-2014

Table of contents

Figures 1-36 and tables 1-2

Figures 37-51 and tables 3-10

List of figures

List of tables

Appendix

Abstract

Object: The aim of this study was to evaluate the effects of the orthopedic treatment (performed either by using active or passive plates) and the subsequent surgical treatment on the palatal size and shape of dental casts of patients with unilateral cleft lip and palate (UCLP).

Material and methods: 96 palatal cast models, obtained from 32 neonatal patients with UCLP, attending the Fundacion Clinica Noel de Medellin (Colombia) were analyzed using a 3D stereophotogrammetric system in three different time points: before the orthopedic treatment, before and after cheiloplasty. Half of the patients were treated with a passive plate, while the other patients received an active plate. The areas and volumes of the greater and minor segments were obtained using a new measurement protocol. Method repeatability both within and between operators was evaluated using the Paired Student's t-test and the technical error of measurement (TEM). Area and volume measurements were compared with a three-way repeated measures analysis of variance (ANOVA) to determine differences between plates, alveolar segments and time.

Results: No systematic measurement errors were found for both inter-operator and intra-operator's tracings ($p>0.05$; TEM<0.32 cm^2). No differences were found for the kind of plates (active or passive). Significant differences were found in alveolar segment and time in both area and volume ($p<0.01$).

Conclusions: We showed that area and volume measurement by the 3D stereophotogrammetric system was a repeatable and reliable method of evaluating the stone casts of patients with UCLP. Data obtained were helpful to quantify changes occurring in maxillary arches of UCLP patients after orthopedic and surgical treatments. However, further investigation is needed to especially evaluate the effects of plates, increasing the number of additional time points and expanding the number of patients.

1- Introduction

1.1- Aim of this study

Non-syndromic orofacial clefts, which include cleft lip, cleft lip and palate and cleft palate alone, comprehend a range of disorders affecting the lips and oral cavity (Mossey et al., 2009). The majority of affected children appear to have low self-esteem, dissatisfaction with their facial appearance and behavioral problems due to their impairment (Mosmuller et al., 2013). To avoid these discomforts, multiple treatments must be planned early in their life.

In order to compare the results of different orthopedical and surgical techniques and to determine optimal timing for lip closure, it is essential to evaluate palatal morphology of several patients during the first 18 months of life.

The purpose of our study was to evaluate the effects of the orthopedic treatment performed by using active or passive plates and the subsequent surgical treatment on the size and shape of the maxillary segments of 32 neonatal patients with cleft lip and palate.

We took into account the changes of the two maxillary segments (greater and minor) during the first year of age in terms of area and volume measurements.

The first step was to find an accurate and reliable method of investigation, assessing the repeatability of both different operators and the same operator over time to calculate the areas of the maxillary segments.

The second step was to compare area measurements of the obtained areas of the maxillary segments during the first year of age, in order to evaluate maxillary growth over time after orthopedic and surgical treatments.

The third step was to compare volume measurements of the maxillary segments over time after orthopedic and surgical treatments.

1.2- Anatomy

1.2.1- The maxillary and the palatine bones

The maxilla forms the upper alveolar process, most of the buccal roof, floor and lateral walls of nasal cavity, orbital floor, part of the infratemporal and pterygopalatine fossae; it delimitates the inferior orbital and pterygomaxillary fissures (fig 1).

Each maxilla has a body and four processes: zygomatic, frontal, alveolar and palatine. The palatine process, thick, strong and horizontal, projects medially from the lowest part of the body of the maxilla, forming a large part of the nasal floor and palate roof. It is much thicker in its anterior part. Its inferior surface is concave and forms the anterior three-fourths of the osseous palate. It displays numerous vascular foramina for palatine vessels and it shows posterolaterally two grooves containing the greater palatine vessels and nerves.

Between the two maxillae the incisive fossa appears behind the incisor teeth. In the fossa there are the orifices of the two lateral incisive canals, that contain the greater palatine artery and nasopalatine nerve (fig 2).

The superior surface of the palatine process is concave transversally, smooth and forms most of the nasal floor; anteriorly near its median border there is the incisive canal. The posterior border is irregular and articulates with the horizontal plates of the palatine bones.

The palatine bones are posteriorly placed between the maxillae and sphenoidal pterygoid processes. Each of them looks like a letter “L” in its horizontal and perpendicular plates, with three processes: pyramidal, orbital and sphenoidal. The horizontal plate is quadrilateral with two surfaces (nasal and oral) and four borders; together with the controlateral bone it forms the posterior quarter of the hard palate. The posterior border is thin and concave behind the palatine crest and gives insertion to the tendon of tensor veli palatine muscle. Medially it forms a posterior nasal spine for the attachment of the uvular muscle (fig 3).

The irregular anterior border articulates with the maxillary palatine process of the same side. The lateral border is continuous with the perpendicular plate. The medial border articulates with the controlateral bone at the midline forming the posterior part of the nasal crest, which articulates with the lower edge of the vomer.

1.2.2- The palate

The palate, or oral roof, is divisible into two parts: the hard palate anteriorly and the soft palate posteriorly.

The hard palate is formed by the palatine processes of the maxillae and the horizontal plates of the palatine bones. In its inferior surface it is bounded anterolaterally by the alveolar arch and gums and it is continuous posteriorly with the soft palate, being covered by a dense mucoperiosteum. It has a median, linear raphe which ends anteriorly in a small papilla over the incisive fossa where the mucosa is thick, pale and corrugated. Posteriorly it is thin, smooth and reddish. Its epithelium is keratinized stratified squamous. There are many palatine mucous glands which lie between the mucosa and the periosteum in its posterior half (fig 4).

The upper surface of the hard palate is part of the nasal floor and is covered by a ciliated respiratory epithelium.

The soft palate slopes down and back between the oral and nasal parts of the pharynx. It is a mobile flap suspended from the posterior border of the hard palate, enclosing an aponeurosis, muscular tissue, vessels, nerves, lymphoid tissue and mucous glands. In its usual position, relaxed and pendant, it has a concave oral surface with a median raphe. Its posterior aspect is convex and continuous with the nasal floor.

Its superior border is attached to the posterior margin of the hard palate and it is connected with the pharyngeal wall. Its inferior border is free, hanging between the mouth and the pharynx. The uvula, a median conical process, projects from its posterior border; the palatal arches, two curved folds of mucosa containing muscular tissue, descend laterally from each side of the uvular base.

The anterior border, called palatoglossal arch, contains the palatoglossus muscle and it descends to the side at the junction of the oral and pharyngeal part of the tongue; it forms the lateral limits of the oropharyngeal isthmus. The posterior border, palatopharyngeal arch, contains the palatopharyngeus muscle and it descends on the lateral wall of the oropharynx. The isthmus of the fauces includes both arches.

Along the median palatine raphe, near the junction between the hard and soft parts of the palate, there are often a pair of depressions. These palatinae foveae may extend into pits, a few millimetres deep, with sagittally elongated openings. They are the common superficial orifices of converging ducts from the palatine mucous glands.

The soft palate mucosa has a non-keratinized, stratified squamous epithelium, except on its upper pharyngeal surface and near the orifices of the auditory tubes, where it is columnar ciliated (respiratory epithelium), as in the nasal cavities.

On both palatal surfaces beneath the mucosa there are palatine mucous glands; they are abundant around the uvula and on the oral aspect of the soft palate, where taste buds also occur.

A thin, fibrous palatine aponeurosis supports the muscles and strengthens the soft palate; it is attached to the posterior border and inferior surface of the hard palate behind the palatine crest. It is thick in the anterior two-thirds of the soft palate but very thin further back. It is composed of the expanded tendons of the tensors veli palatini muscle; near the midline it encloses the musculus uvulae. All the other palatine muscles are attached to it.

The arteries of the palate are the greater palatine branch of the maxillary artery, the ascending palatine branch of the facial artery and the palatine branch of the ascending pharyngeal artery. The veins end largely in the pterygoid and tonsillar plexuses. The lymph vessels pass to the deep cervical lymph nodes.

The sensory nerves issue from the greater and lesser palatine, nasopalatine and glossopharyngeal nerves; the lesser palatine nerve contains taste fibres from the oral surface of the soft palate.

1.2.3- Palatine muscles

The palatine muscles include: the levator veli palatini, tensor veli palatini, palatoglossus, palatopharyngeus and musculus uvulae (fig 5).

1-The levator veli palatine is cylindrical and lies lateral to the posterior nasal aperture. It is attached:

-By a small tendon to a rough area on the inferior surface of the petrous part of the temporal bone in front of the lower opening of the carotid canal.

-By muscle fibres to a sheet of fascia descending from the tympanic vaginal process to form the upper part of the carotid sheath.

-By a few fibres to the inferior aspect of the cartilaginous part of the auditory tube.

It crosses medial to the auditory tube at the level of the medial pterygoid lamina. It spreads in the soft palate between the two strands of the palatopharyngeus, passing above the upper margin of the superior constrictor pharyngis and in front of the salpingopharyngeus. Its fibres are attached to the upper surface of the palatine aponeurosis as far as the midline where they blend with those of the contralateral muscle. The levator veli palatini elevates the soft palate.

2-The tensor veli palatini, a thin, triangular muscle, is lateral to the medial pterygoid plate, auditory tube and levator veli palatine. Its lateral surface contacts the upper anterior part of the medial pterygoid, the mandibular, auriculo-temporal and chorda tympani nerves, the otic ganglion and the middle meningeal artery.

It is attached to the scaphoid fossa of the pterygoid process, to the lateral lamina of the cartilage of the auditory tube and to the sphenoidal spine. Its fibres descend and converge into a delicate tendon turning medially round the pterygoid hamulus and pass through the origin of the buccinator

to the palatine aponeurosis and the osseus surface behind the palatine crest on the horizontal plate of the palatine bone. Between the tendon and the pterygoid halamus there is a small bursa.

The muscle pulls the soft palate to one side alone and with the controlateral it tenses the soft palate (principally its anterior part), depressing it by flattening its arch.

3-The palatoglossus is a small muscular fasciculus narrower at its middle than at its ends and it forms, including the mucosa, the palatoglossal arch.

From the oral surface of the palatine aponeurosis, where it is continuous with the controlateral, it extends antero-inferiorly and laterally in front of the tonsil to the side of the tongue, some of its fibres spreading over the lingual dorsum, other passing deeply into its substance to intermingle with the transversus linguae.

The palatoglossus elevates the root of the tongue and approximates the palatoglossal arch to the midline, thus shutting off the oral cavity from the oropharynx.

4-The palatopharyngeus muscle forms, with its overlying mucosa, the palatopharyngeal arch. In the palate its two fasciculi are separated by the levator veli palatini muscle.

The posterior fasciculus is in contact with the mucosa of the pharyngeal aspect of the palate; it joins in the midline its contralateral one. The thicker anterior fasciculus passes between the levator and tensor veli palatini and is attached to the posterior border of the hard palate and to the palatine aponeurosis, some fibres interdigitating with the controlateral across the midline. Both fasciculi are attached to the upper aspect of the palatine aponeurosis. At the posterolateral border of the soft palate the two layers are joined by fibres of salpingopharyngeus.

Passing laterally and downwards behind the tonsil, the palatopharyngeus descends posteromedial to the stylopharyngeus, to be attached with it to the posterior border of the thyroid cartilage; some fibres end on the side of the pharynx and others cross the midline posteriorly, mixing with those of the opposite site muscle. The palatopharyngeus thus forms an incomplete internal longitudinal muscular layer in the wall of the pharynx.

The palatopharyngei muscles pull the pharynx up, forwards and medially, shortening it during swallowing. They also approximate the palatopharyngeal arches drawing them forwards.

5-the musculus uvulae, a bilateral structure, is attached to the posterior nasal spine of the palatine bone and to the palatine aponeurosis. It descends to be inserted into the uvular mucosa.

The muscle allows the elevation and retraction of the uvula.

Except for tensor veli palatini, which is innervated by the mandibular nerve, all the palatine muscles are supplied by nerve fibres which leave the medulla in the cranial part of the accessory nerve and reach the pharyngeal plexus via the vagus nerve.

In the soft palate the muscles are arranged as follows: the palatine aponeurosis (tendon of the tensores veli palatini) is intermediate, enclosing the uvular muscles near the midline; the levatores

veli palatini and palatopharyngi are attached to its upper surface, the two fasciculi of the latter separated by the former; the palatoglossi are attached to the inferior surface of the aponeurosis.

1.2.4- The lips

The lips are two fleshy folds around the oral orifice, formed externally by skin and internally by a mucous membrane enclosing the orbicularis oris muscle, labial vessels and nerves, fibroadipose connective tissue and numerous small labial salivary glands secreting into the oral cavity (fig 6).

On each side a labial commissure forms the angle of the mouth, usually in correspondence of the first premolar tooth. In the central part of the cutaneous surface of the upper lip there is a shallow vertical groove, the philtrum, ending below in a slight tubercle and limited by lateral ridges. The mucous surface of each lip is connected to the gum by a median labial frenulum, the upper being the larger (fig 7).

The labial glands, situated between the mucosa and the orbicularis oris muscle, are about the size of small peas and in structure they resemble mucous salivary glands. Their ducts open into the oral vestibule (fig 8).

1.3- Embryology

1.3.1- The face, nasal cavity and palate

During the fourth week of development, the stomatodeum or primitive mouth is bounded cranially by the forebrain and caudally by the cardiac prominence.

During the fifth week, while the mandibular prominence caudally is invading the floor of the pharynx, the epithelial roof of the primitive mouth proliferates to form the two frontonasal prominences. They consist of mesenchyme covered by ectoderm. A plaque of ectoderm develops on each side dividing the frontonasal prominence into the medial and lateral nasal prominences, also named nasal placodes. They soon become depressed to form the olfactory pits or nasal sacs (fig 9).

The two medial nasal prominences, still separated by the medial portion of the frontonasal field, project into the roof of the stomatodeum to form the premaxillary or globular fields. While these changes are progressing, a somewhat triangular elevation swells ventrally on each side; this is the maxillary prominence and it consists of proliferating mesenchyme covered by ectoderm.

It fuses with the lateral nasal prominence (the two at first are separated by a groove, the naso-optic furrow), the two structures grow together to establish continuity between the future nose and the cheek.

During the eighth week, the relatively wide primitive mouth or stomatodeal fissure is progressively reduced while the epithelial and connettive tissues of the cheek enlarge by fusion between the adjacent surfaces of the mandibular and maxillary prominences (fig 10).

The growth of the maxillary prominence, which extends beyond the lateral nasal prominence to fuse with the premaxillary elevation, leads to a deepening of the nasal pit to become a primitive nasal cavity or nasal sac, the epithelial wall of which is the nasal fin. It retains contiguity with the epithelium of the stomatodeal roof. Subsequently the nasal fin is eroded forming a thin layer, the oronasal membrane, which disappears later.

The primitive nasal cavity communicates with the stomatodeum through a primitive internal naris (choana) which is ventrally situated in the stomatodeal roof. By this change a new cranial boundary is set for the oral opening, consisting of the fused premaxillary and maxillary regions. This is the future upper lip, but it has not yet become separated from the deeper tissues which will form the maxillary alveolus.

At the same time the nasal cavity acquires a floor through the fusion of the nasal and the maxillary prominences of each side. At this stage the two external nares are still widely separated but this separation becomes reduced by the fusion, during the eighth week, of the mesenchyme of the maxillary prominences. This mesenchyme contributes to the formation of the philtrum of the upper lip.

The maxillary nerve innervates the philtrum and it extends later into the territory of the frontonasal prominence.

1.3.2- The palate

The roof of the oral cavity (primitive palate) is formed by the premaxillary regions and the maxillary prominences which become confluent and establish continuity with the thick median nasal septum. The broad dorsocaudal border of the nasal septum is, at first, in contact with the dorsum of the developing tongue and the right and the left nasal cavities still communicating freely with the mouth except where the nasal floor is already established ventrally by the primitive palate (fig 11).

During the sixth week (fig 12), the maxillary prominences produce the palatine processes which grow towards the midline but are for some time separated from each other by the tongue (fig 13). At this stage the roof of the oral cavity projects ventrally beyond its floor and the tip of the developing tongue actually lies in contact with the superior face of the primitive palate. At the same time (sixth week), the two palatine processes bend into a vertical position on each side of the tongue

but slightly after the tongue is carried forwards and the two palatine processes assume a horizontal position which allow them to grow towards each other and thus to fuse (fig 14).

This change of position occurs very rapidly in animal and human palate and the event may have a direct bearing on the maldevelopment of the palate.

During the eighth week the development of the neck, allowing some descent of the tongue and of the floor of the mouth, is also occurring and produces the palatal elevation. This permits the palatine processes to grow medially along the inferior borders of the primitive choanae, fusing with them except over a small area in the midline where the nasopalatine canal maintains connection between the nasal and the oral cavities and marks the future position of the incisive fossa (fig 15).

As the borders of the maxillary palatine processes fuse together, fusing also with the free border of the nasal septum, the nasal and oral cavities are progressively separated. The nasal cavities extend dorsally and reach their final position leaving the nasal septum free in its dorsal quarter as the partition between them.

Slightly later the dorsomedial extremities of the palatine processes fuse together rostrocaudally to form the future soft palate. This fusion is more apparent than real, in fact the epithelial cleft between them being pushed to the surface by mesenchymal growth.

1.3.3- Anomalies: developmental bases

Congenital malformations consequent to the arrest of development and failure of fusion of components in the formation of the face are not uncommon. At the simplest one maxillary prominence may fail completely to fuse with the premaxillary region leading to a persistent fissure between the philtrum (fig 16 and 17) and the lateral part of the upper lip on that side (cleft lip).

A similar rare malformation follows the failure of fusion between the maxillary prominence and the lateral nasal prominence (facial cleft), in which the nasolacrimal duct persists as an open furrow.

The palatine processes may fail to fuse with each other and the nasal septum to variable degrees. In its severest form the fusion is wholly lacking leaving a wide fissure through which the nasal septum is visible. On each side the premaxillary parts of the palate are separated from the maxillary palatine processes by clefts which are continuous ventrally with bilateral clefts in the upper lip. The floor of the nasal cavity is deficient throughout its extent and the choanae are not completed.

Many varieties of milder degrees of cleft palate have been observed: the commonest type is unilateral, only one side of the nasal cavity being in communication with the mouth and the extent of the cleft being variable (fig 18). In the mildest form only the soft palate is cleft.

Such examples of arrested development may be associated with disturbances in embryonic nutrition during the second and the third months of gestation and the grosser varieties are usually coupled with malformations in other regions of the body.

Certain midline anomalies are rarely encountered, median cleft lip (true hare lip), cleft nose and cleft lower jaw. More common are minor degrees of cleft chin and micrognathia (under-development of the lower jaw).

1.4- Cleft lip and cleft palate

1.4.1- Clinical aspects

Every year an estimated 7.9 million children, 6% of total births worldwide, are born with a serious birth defect of genetic or partly genetic origin.

Between 44% and 60% of congenital anomalies affect the craniofacial structures and the most common group of craniofacial anomalies is orofacial clefts (OFC).

Orofacial clefts are the second most common birth anomaly after clubfoot (de Ladeira and Alonso, 2012)

In 2001 an International Database on Craniofacial Anomalies (IDCFA) was created with the primary aim to establish a single database for the collection of existing and new information on craniofacial anomalies from around the world (Mossey, 2007; Mossey et al., 2009).

Cleft lip and cleft palate are among the most commonly occurring congenital craniofacial defects with approximately one in 500-700 newborn babies affected worldwide (Bugaighis et al., 2013). Combined cleft lip and palate is the most common presentation (50%), followed by isolated cleft palate (30%), isolated cleft lip (20%) and least common is cleft lip and alveolus (5%) (fig 19) (Young, 1998).

1.4.2- Geographical distribution and ethnicity of oral facial clefts

Descriptive epidemiology using IDCFA database confirmed the apparent correlation between frequency of orofacial clefts and latitude in Europe ($r = 0.69$) with a progressive increase in Finland and Norway and of orofacial clefts and longitude with an increasing frequency from East to West in North America ($r = 0.67$).

For cleft lip with or without cleft palate, the highest recorded rates are found in Far East, India, Japan, Aborigines, Scandinavia, Native Americans and parts of South America, while the lowest rates in Africa, Southern Europe and African Americans (Mossey, 2007).

Conversely the rate of isolated cleft palate is constant among ethnic groups with less geographical variation than cleft lip and palate (fig 20, tab 1).

1.4.3- Gender, cleft type and laterality

Clefts of the lip and combined lip and palate are twice as common in males, while isolated cleft palates are twice as common in females. Also the male excess in cleft lip and palate is more apparent with increasing severity of the cleft.

Unilateral clefts form 80-85% of all CLP cases and two-thirds of these have left-sided clefts regardless of sex, race and severity of the defect.

A possible explanation is that blood vessels supplying the right side of the foetal head leave the aortic arch closer to the heart and perhaps are better perfused by blood than those going to the left side.

1.4.4- Evidence for possible environmental influence

The highest rates of clefts were observed in areas of high unemployment and poor housing but there are difficulties in defining what exactly contributes to low socioeconomic status. This could be a combination of known environmental factors as maternal smoking, maternal illness and infections (rubella virus), occupational exposure, alcohol consumption, differences in nutrition, medications (thalidomide and aminopterin) or drugs.

Maternal diabetes mellitus and amniotic band syndrome are associated with clefts. Increased paternal, but not maternal age, is also associated with clefts.

1.4.5- Genetic epidemiology

Nonsyndromic inheritance of facial clefting is multifactorial. Familial inheritance of both cleft lip and palate occurs with varying frequency, depending on whether a parent or sibling is affected. For cleft lip with or without cleft palate, the risk rate for future offspring is 2% with only one parent affected,

4% with only one sibling affected, 9% with two siblings affected, and 10-17% with one parent and one sibling affected. For cleft palate alone, the risk rate for future offspring is 7% with only one parent affected, 2% with only one sibling affected, 1% with two siblings affected, and 17% with one parent and one sibling affected.

Chromosome aberrations such as trisomy D and E have increased incidence of clefts. Facial clefts are associated with a syndrome 15-60% of the time. More than 200 recognized syndromes may include a facial cleft as a manifestation. Common syndromes with cleft palates include Apert's, Stickler's and Treacher Collins. Van der Woude's and Waardenberg's syndromes are associated with cleft lip with or without cleft palate (Young, 1998).

Although significant progress has been made in understanding the genetic etiology of syndromic orofacial clefting, the identification of genetic variants has progressed at a slower pace due to its multifactorial nature. A key to understand the etiology of clefts lies in discerning the complex spectrum of subphenotypic expression of this condition, not only in individuals presenting overt clefts, but also in their seemingly unaffected close relatives with whom they share a portion of their genome. Studies have shown that unaffected relatives of individuals with clefts present narrower cranial vaults, longer cranial bases, wider, shorter and more retrusive upper faces, longer and more protrusive lower faces, wider soft tissue noses and wider nasal cavities than controls (Otero et al., 2012). The affected individuals present decreased vertical and anterior-posterior dimensions in the maxilla, downward and backward rotation of the mandible with a very steep mandibular plane, reduced posterior facial height and increased anterior facial height giving the appearance of bimaxillary retrusive faces. These data support the presence of distinct facial morphology in cleft risk carriers.

In addition to these morphometric studies, other research has also been done to examine the presence of asymmetry in facial and dental traits. Dental abnormalities including bilateral asymmetrical expression of missing teeth have been found more often in individuals with clefts than in controls.

The categories of candidate gene classes for orofacial clefts comprehend transcription factors, growth factors, cell signalling molecules, folate pathway genes and detoxification enzymes.

The identification of chromosomal breakpoints and deletions is an important example of recent success with the discovery of the SATB2 gene which is a plausible location for a polymorphism causing isolated cleft palate (Mossey, 2007).

A complete list and description of craniofacial candidate genes involved in clefting is shown in tab 2**.** For example the genes PITX2, ISL1 and SNAI1 have very specific roles during the formation of the lip, palate and anterior teeth as well as for facial expression and for masticatory muscles (Miller et al., 2014).

The new diagnostic tool, comparative genomic hybridization (Array-CGH), which enables the detection of microdeletions, may become a routine method of genome-wide screening in children with CP and perhaps also CLP.

1.5- Clinical examination

The development of oral cleft can compromise the functional (feeding, hearing, speaking, swallowing, breathing), the social (dissatisfaction with facial appearance, behavioral problems) and the psicological well-being (low self-esteem) of affected people and can adversely affect their and their families' quality of life (Papamanou et al., 2012).

A team approach is needed to manage the wide variety of problems common to the patient and family with cleft lip and palate. In addition to the reconstructive surgeon, a typical team consists of an otolaryngologist, a dentist, a speech pathologist, an audiologist, a geneticist, a nurse, a psychiatrist, a social worker, a prosthodontist and an orthodontist.

These specialists perform a complete head and neck examination on new patients in the cleft palate clinic.

The head is inspected for symmetry, the auricle and external canal for development and location.

A facial analysis is helpful to identify abnormalities of facial symmetry and harmony.

The otolaryngologist performs the otologic examination which includes pneumatic otoscopy and tuning forks. Anterior and posterior rhinoscopy will identify clefting, septal abnormalities, intranasal masses and choanal atresia.

The dentist performs the oral cavity examination by identifying any cleft, dental arch abnormalities and tongue anomalies such as bifid tongue, macroglossia, glossoptosis or lingual thyroid. In addition malocclusion, hemifacial hypertrophy or atrophy and facial clefting are documented.

The upper airway tract is evaluated by assessing the adequacy of phonation, cough, deglutition and by auscultating and palpating the neck.

1.5.1- Speech disorders

Errors in articulation are common in cleft palate patients, especially those involving affricates and fricatives. Other errors include stop, glides and nasal semivowels.

Velopharyngeal incompetence is associated with an audible escape of air from the nose during production of pressure sounds and is termed nasal emission or snort. It is estimated that 75% of patients have velopharyngeal competence following primary cleft palate surgery and this can be increased to 90-95% with directed secondary procedures. Velopharyngeal competence is the most important determinant of articulation performance and listener understanding of speech in cleft palate patients. Other factors include dentition, associated hearing loss, muscular and neurologic

deficits. Velopharyngeal competence can be estimated by direct examination of the nasopharyngeal depth, palatal length and palate movement during phonation.

1.5.2- Ear diseases

Patients with an isolated cleft lip have an incidence of hearing loss similar to that in the normal population. In contrast, cleft palate is very often associated with Eustachian tube dysfunction and a resulting conductive hearing loss. Eustachian tube dysfunction in these patients is due to an abnormal insertion of the levator and tensor veli palatine muscles into the posterior margin of the hard palate. In addition to middle ear effusion, the patients also appear to have an increased incidence of cholesteatoma (7%). With increasing age, the incidence of Eustachian tube dysfunction decreases and in many cases normal Eustachian tube function develops by mid adolescence. Otologic goals in the cleft palate patient are to provide adequate hearing, maintain ossicular continuity and adequate middle ear space and prevent deterioration of the tympanic membrane. Indications for myringotomy and tube insertion include a significant conductive hearing loss or persistent middle ear effusion, recurrent otitis media or tympanic membrane retraction.

1.5.3- Airway problems

Airway problems may arise in children with cleft palates, especially those with concomitant structural or functional anomalies. For example, Pierre-Robin sequence is the combination of micrognathia, cleft palate and glossoptosis. Affected patients may develop airway distress from their tongue becoming lodged in the palatal defect (Young, 1998).

1.6- Treatment

1.6.1- Orthopedic treatment

It is important to treat the cleft as soon as possible to guarantee a correct growth of the baby otherwise the patient could face several difficulties in feeding, hearing, speaking, swallowing, breathing and have a high risk of chronic otitis (due to the presence of fluids in the Eustachian tubes coming from nasal cavity).

As already stated, a team approach is fundamental. The treatment of cleft lip and palate consists of orthopedics and of multiple surgeries (Mosmuller et al., 2013). In fact, before performing surgery,

part of the treatment protocol in many centers includes infant orthopedics (Papadopoulos et al., 2012), used to actively align the segments to facilitate surgery (by reducing the gap to be closed), to normalize tongue position, to mould the growth of the alveolus, to create an optimal condition for the configuration of maxillary segments and to facilitate feeding (Yamada et al., 2003). Infant orthopedics can be performed with active and passive acrylic plates (fig 21).

Since the very first days of life the orthodontist takes an impression of the maxilla (fig 22) in order to obtain an acrylic plate. The plate can be checked and modified every 15 days so that it can actively guide the growth of the two segments.

This approach allows a more normalized pattern of deglutition, prevents twisting and dorsal position of the tongue in the cleft, improves arch form and position of the alar base and facilitates surgery, flattens the palatal shelves, prevents cross-bites, straightens the nasal septum, allows a better speech development, a better nose breathing, a better middle ear condition and renders a favorable facial growth. Because of these positive effects less speech therapy and orthodontic treatment is assumed to be needed in the long term (Prahl et al., 2001).

1.6.2- Repair of cleft lip (cheiloplasty)

The first performed operation is the surgical repair of the lip (cheiloplasty), which is usually performed between 10 and 24 weeks of age.

Lip adhesions can also be performed at 2 weeks of age to convert a complete cleft to an incomplete cleft and serve as a temporary measure for those infants with certain feeding problems. Nevertheless adhesions may interfere with definitive lip repair and are less often needed in recent years due to the wider variety of specialty feeding nipples available.

Surgical correction has evolved (Demke and Tatum, 2011) from straight-line repair as described by Rose in 1891 and Thompson in 1912. Their techniques involved the use of angled incisions made at the opposing cleft margins. These curvilinear incisions along the cleft margins were used to gain vertical lip length, the medial lip is rotated down and the incisions straightened out. There is potential for scar contracture and sacrifice of excess normal tissues (fig 23).

Tennison in 1952 and Le Mesurier in 1955 started a more sophisticated repair with preservation and positioning of the cupid's bow. Their repairs were the most widely used techniques, however they could not avoid the presence of contractures in post-operative times (fig 24).

The Millard procedure, presented in 1957, entails lateral flap advancement into the upper portion of the lip combined with downward rotation of the medial segment. This technique involves back-cuts placed along the medial lip cleft side philtral ridge and one or more lateral lip-element triangular advancement flaps to fill in the resultant defect as the medial lip element is rotated down.

The main disadvantage of Millard's repair is that one can get a vertical scar contracture with vermilion notching of the lip or lowering of the alar base (fig 25).

Since its introduction by Millard, the rotation advancement flap lip repair has undergone a great number of modifications by different authors.

In 1993 Nakajima raised a triangular flap at the alar base on the cleft-side and advanced it to the bottom of the columella achieving a straight suture line.

In 2012 Zayed introduced the concept of junctional zones in unilateral cleft lip repair where the lip is classified into cutaneous portion and vermilion. The cutaneous portion is subdivided into main zone and flat zone by three lines (1, 2, 3 in fig 26). The vermilion is subdivided into dry zone and transitional zone by two lines (4, 5). Line 1 represents the lip-columellar junction of the philtrum and alar lip junction of the cleft-side. Line 2 lies between the flat and main cutaneous portions of the upper lip. Line 3 is the vermilion-cutaneous junctions "white roll". Line 4 is a vermilion ridge between dry zone and transitional zone of the vermilion. Line 5 is the red line between the vermilion and oral mucosa (fig 27).

The rotation advancement principles are used for the upper part of the main zone and the Z plasty is used for the lower part of the main zone. Straight line closure is used for the flat cutaneous zone and dry vermilion. The laterally based mucosal flap is used for the transitional vermilion to repair the vermilion deficit on the medial side of the cleft (Zayed et al., 2012).

1.6.3- Repair of cleft palate (palatoplasty)

It was usually performed between the age of 10 to 24 months, but currently it is anticipated even at the age of 3 months (sometimes together with cheiloplasty).

Several techniques for cleft palate repair have been developed over the past three decades. Until 1969 the "push-back" technique by Veau Wardill Kilner (lengthening the back of the palate) was the most popular one (fig 28). The current trend is toward procedures that involve less denuding and scarring of the hard palate and less tension on the soft palate (like Furlow double-opposing z-plasty).

The two-flap techniques, such as those described by Bardach or Furlow are commonly used. Furlow z-plasty increases palatal length at the expense of width and correctly reorients the levators and palatopharyngeus muscles, thus thickening the velum (fig 29).

In Bardach's repair a single posteriorly based mucoperiosteal flap is developed over each palatal shelf. In this repair medial incisions are made to separate the oral and nasal mucosa and lateral incisions are made at the junction of the palate and alveolar ridge. The mucoperiosteal flaps are elevated, taking care to identify and preserve the neurovascular bundle containing the greater palatine artery. Next, the velar muscle is detached from its attachment to the posterior border of

the palatal shelves. The palate is then closed in three layers, the first is the nasal mucosa, then the velar muscle and finally the oral mucosa. The lateral palate incisions are closed loosely.

Bilateral cleft palate repairs are performed in a similar way.

Although controversial, many authors believe there is a relationship between scar formation of the palatal repair and the impaired mid-facial growth that is observed in most patients with cleft palate. Bony abnormalities that develop include collapse of the alveolar arches, midface retrusion and malocclusion.

Some surgeons advocate late repair, because facial growth is less affected when surgery is delayed until 18-24 months of age. Others advocate an earlier repair, stating that feeding, speech and socialization are improved if the surgery is performed by the first year of life and that facial growth problems can be minimized with less traumatic palate repairs.

Cleft palate patients at high surgical risk or who refuse surgical treatment may use a dental obturator to obtain velopharyngeal competence. Disadvantages of dental obturators include the necessity of wearing a prosthesis and the need for modification of the prosthesis as the patient grows.

1.6.4- Orthodontic treatment

In deciduous dentition, between the age of 4 to 6 years, the orthodontic treatment must be performed only in case of lateral (insufficiency of the superior transverse diameters) or anterior (underdeveloped maxillary with severe skeletal Class III) cross-bites (Corbo M et al., 2005). These shortcomings are basically due to the scarring after cheiloplasty and palatoplasty.

Orthodontic appliances like quad-helix or rapid palatal expander (fig 30 and 31) can grant the right expansion in the transverse diameters and ensure space to facilitate the correct dental eruption in particular close to the cleft (Muchitsch et al., 2012). Delaire mask can correct severe skeletal Class III (fig 32).

In mixed dentition, between the age of 6 and 12 years, the orthodontic treatment still aims to correct the insufficiency of the superior transverse diameter and the growth trend in Class III, but also focuses on the agenesis, supernumerary teeth and malposition of teeth close to the cleft.

To overcome these dental defects, orthodontic brackets can be placed on the malpositioned teeth and on the other permanent teeth to achieve an early proper alignment and guide the correct development of the remaining erupting teeth (fig 33).

Bone graft to close the cleft is usually performed before maxillary canine eruption (9-11 years) so that its eruptive path is facilitated.

In permanent dentition, usually after 12 years, brackets are placed to align the teeth. However in cleft patient the permanent teeth eruption is delayed especially in the cleft-side in comparison to the unaffected one so the orthodontic treatment is often postponed (fig 34). Missing teeth can be replaced with prostheses.

Orthodontic appliances cannot always correct the skeletal discrepancy. In case of severe discrepancy, the presurgical orthodontic preparation aims at removing all dental compensations looking forward to the sagittal osteotomy of the mandible and maxillary advancement surgery when facial growth is completed (Altug-Atac et al., 2008; Gandolfini et al., 1993).

1.7- Previous studies about palate measurement

1.7.1- From conventional to digital measurements

Hard palate and dental arch morphology is usually studied using stone casts which accurately reproduce their three-dimensional characteristics.

The quantitative analysis of dental casts (for instance the dimensions of the palate and the relative positions of the teeth) was usually performed by direct techniques: several standardized landmarks were individualized on the cast and the measurement were taken directly on the model using calipers (Ladner and Muhl, 1995).

This method was time-consuming because each measurement had to be made directly on the cast and the landmarks had to be individualized several times, thus incrementing the possible errors. Moreover the landmark coordinates cannot be digitized and no data banks for future measurements could be obtained.

A different method to analyze the dental arches and the palate was the individualization of the landmarks on photographic or radiographic prints. These landmarks could be then digitized with an electromagnetic tablet. The digitization of two-dimensional landmarks overcame some of the limits of the direct approach, but the third dimension was lost. Indeed, all the three dimensions are duly necessary for a proper quantitative analysis of the palate.

Luckily new dental impression materials and casting techniques as well as new three dimensional digitizers together with the use of computer facilities offered the possibility of extensive and accurate three-dimensional morphometric evaluations (Braumann et al., 1999; Ferrario et al., 1994). Therefore data can be digitized, collected in banks and compared with future studies.

Berkowitz used an electromechanical instrument which quantitatively described palatal growth in small samples of both normal and cleft palate patients by measuring the palatal surface area, several dental and anthropometric distances, as well as the cleft spaces. Other authors instead used three-dimensional digitizers to study dental arches in terms of mathematical shape (Berkowitz, 1999).

The studies by Ferrario et al. (1994, 1998) devised a mathematical equation of palatal shape with curve fitting algorithms independent of the size. They collected a set of landmarks from the stone casts using a three-dimensional computerized device (Colombo et al., 2001). This three-dimensional digitizer (3Draw, Polhemus Inc., Colchester, VT, USA) is an electromagnetic device interfaced with a computer. The system has a resolution of 0.0005 cm/cm of range, and is usually calibrated before each data-collection session, thus supplying real metric data independent from external reference systems (Ferrario et al., 1997).

The electromagnetic digitizer can overcome the shortcomings of the two dimensional projection: the loss of the third dimension does not influence dental arch form in the horizontal plane but in hinders most investigations of palatal morphology. The metric coordinates of landmarks can be obtained also by optical devices and electromechanical instruments. The coordinates can then be used for any kind of mathematical modeling.

In the mathematical model devised by Ferrario et al. (1994), palatal shape (size independent) was assessed by four-order polynomials in the sagittal and frontal plane projections.

In further studies Ferrario and coworkers analyzed the effect of age (children, adolescents and adults) and sex on the form (size and shape) of hard tissue palate in normal Italian individuals. A complete set of data regarding hard-tissue palatal dimensions in children three to six years of age was obtained (Ciusa et al., 2007). Palatal dimensions in the frontal and sagittal planes were compared between ages and sexes, showing changes in the palatal widths (Ishida et al., 2013) even once the permanent dentition was established, especially in males (Ferrario et al., 2001), but a longitudinal assessment showed no significant changes in hard tissue palatal size between twenty and thirty years of age in healthy normal men and women (Ferrario et al., 2002).

Ethnicity seems to be a factor of major variability of human hard palate morphology according to some studies (Burris et al., 1998; Byers et al., 1997), even if no differences were found among three groups of Chilean people with different ethnic compositions (Ferrario et al., 2000).

Further studies to evaluate palatal morphology were performed in patients with different disorders: ectodermal dysplasia (Dellavia et al., 2006), Down syndrome (Dellavia et al., 2007), bruxist children (Restrepo et al., 2008).

The following landmarks were originally taken into account by Ferrario et al. in their first studies and were also used in the following studies with some modifications (fig 35):

1-The intersections of the palatal sulci of the left and right first permanent molars with the gingival margin (MR –ML).

2-The incisive papilla (IP).

3-The posteriormost limit of the palatal raphe (RP).

4-The intersection between the intermolar line and the papilla perpendicular (M).

All palates were oriented according to a common intrinsic orientation, by setting the following planes:

1-Horizontal plane: incisive papilla and left and right molar points.

2-Sagittal plane: palatal length, horizontal projection of the distance between the incisive papilla and the sagittal molar point.

3-Frontal plane: palatal width at the first permanent molars.

1.7.2- Optical scanners

Other authors proposed the use of an optical three-dimensional digital system (Braumann et al., 1999). Optical instruments are basically stereophotogrammetry and laser scanner. Laser scanners provide a detailed analysis of objects based on clouds of points obtained by projecting a laser light over them. The reflected light is recorded by a camera interfaced with a computer and transformed in 3D information using triangulation geometry.

Laser scanning is a noninvasive technique and it offers a computerized data collection, but it is more expensive and slower than stereophotogrammetry. Also, it usually does not provide a photographic recording of the object and it does not allow the operator to directly identify the landmarks on the object.

Stereophotogrammetry uses two or more images to create a three-dimensional one. It combines the benefits of conventional anthropometry and computerized photographic or laser systems (Ferrario et al., 2003).

In fact, as the laser scanner, stereophotogrammetry is a noninvasive, but expensive technique. It offers a computerized data collection as well, but it also provides high-resolution photographic images. Its major disadvantage is the difficulty to record hidden surfaces and undercuts.

Recently, stereophotogrammetry has been used to analyze cast of patients with cleft lip and palate (Sforza et al., 2012). Three-dimensional measurements (cleft width, depth and length) were made separately for the longer and shorter segments on the digital dental cast surface between previously marked landmarks (fig 36). These landmarks were identified both in the greater and in the minor segment according to the studies by Prahl et al. (2001) and Yamada et al. (2003):

-Postgingivale: posterior endpoint of the alveolar crest at the junction of the crest of the ridge with the outline of the tuberosity (Pg on the greater segment, Pm on the minor segment).

-Anterior alveolar: anterior endpoint of the alveolar crest where the continuation of a line marking the crest of the ridge turns from the oral side to the nasal side at the anterior end of the segment (Ag on the greater segment, Am on the minor segment).

-Canine: crossing point of the canine groove and alveolar ridge (Cg on the greater segment, Cm on the minor segment).

-Deep cleft: deepest point of the cleft (Dg on the greater segment, Dm on the minor segment).

The study compared three-dimensional stereophotogrammetry with conventional caliper measurements. The procedure consisted of the digitization of palatal casts using a 3D stereophotogrammetric system (Vectra 3D Canfield Scientific, Fairfield NJ) and data obtained were analyzed using the stereophotogrammetric software (de Menezes et al., 2010).

Only linear distances among the landmarks previously described were measured with the “point to point” distance tool of the stereophotogrammetric software and compared with the same measurements obtained by the caliper. Significant systematic errors were found. Caliper measurements were larger than 3D stereophotogrammetric ones for distances: Pg-Pm, Am-Pm, Dm-Cm and Dg-Cg and lower for distances Ag-Am and Ag-Pg.

The differences found between the two measurement methods were in agreement with previous studies that performed linear measurements between reference points with digital calipers directly on cast models (Naidu et al., 2009) and were clinically negligible: overall, also considering method errors and time necessary for the analysis, measurements recorded by the 3D stereophotogrammetric system appeared to be reliable (Sforza et al., 2012) for assessing stone casts of newborn patients with unilateral cleft lip and palate (UCLP).

Figures

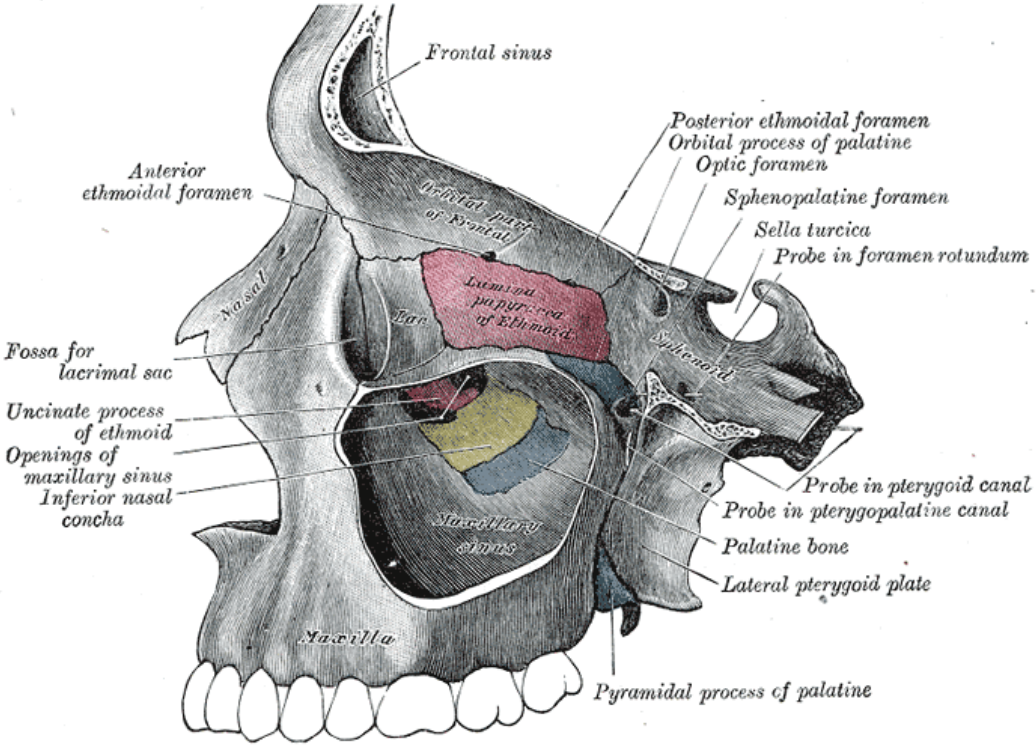

Fig 1. **Left maxillary sinus opened from the exterior showing the medial wall of the left orbit and the medial wall of the left maxillary sinus (Gray, 1918).**

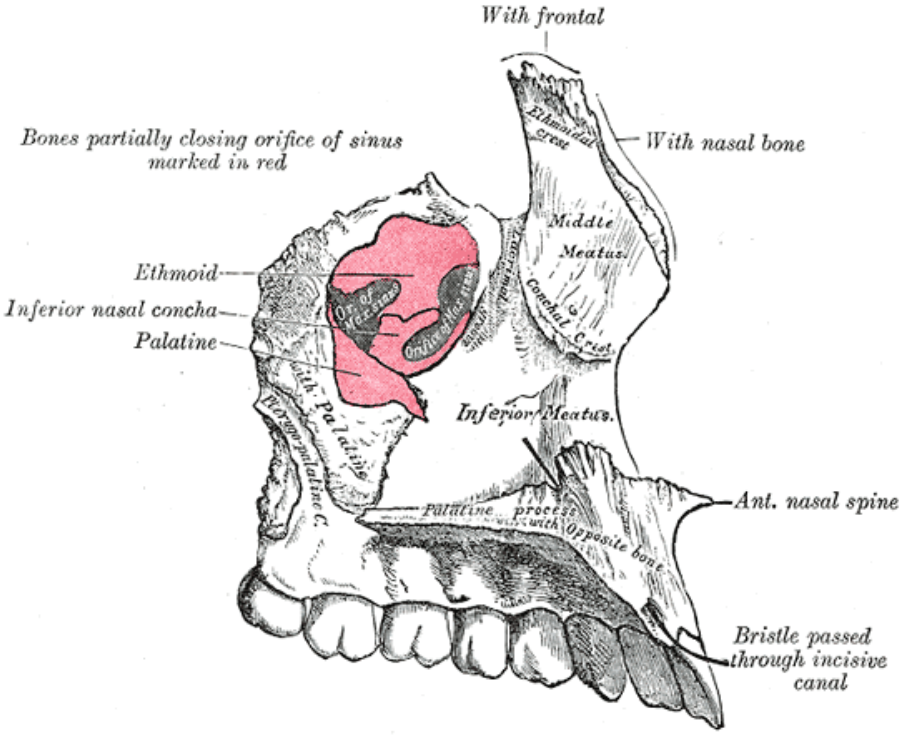

Fig 2. **The left maxilla: medial aspect (Gray, 1918).**

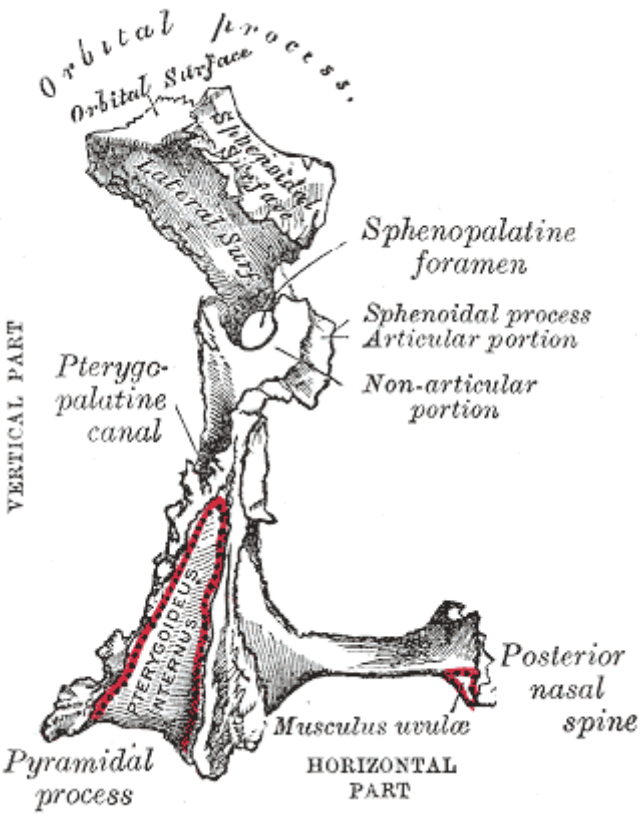

Fig 3. **The left palatine bone: posterior aspect (Gray, 1918).**

Fig 4. **The hard palate.**

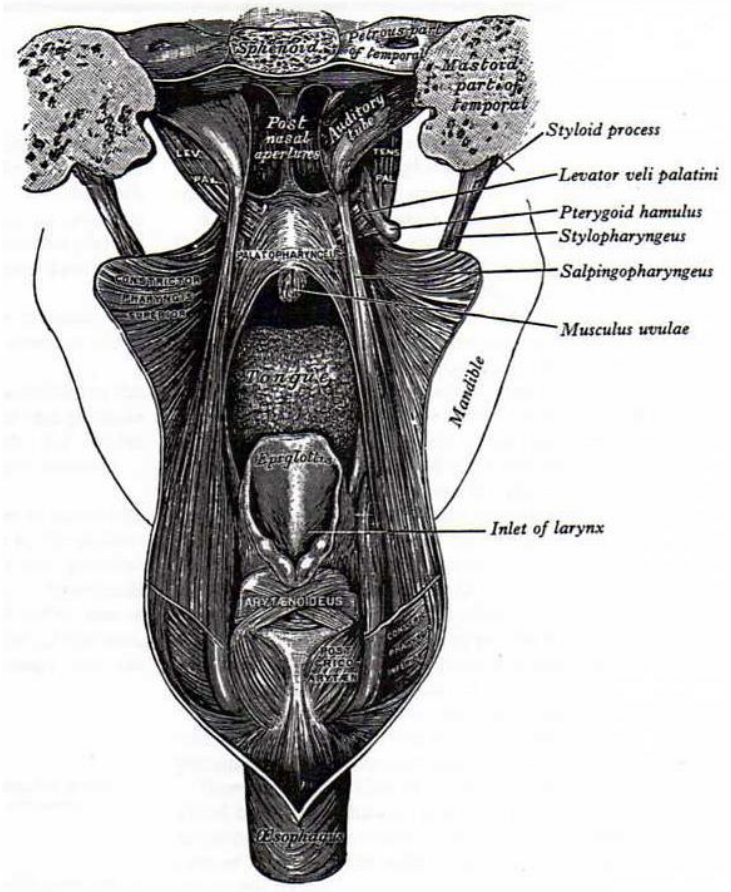

Fig 5. **The muscles of the palate, exposed from the posterior aspect (Williams et al., 1989).**

Fig 6. **The lips: external view**

Fig 7. **Mucous surface of the lips**

Fig 8. **Cross-sectional area of the lip. On the left: the outer part; on the right: the inner part (Penna et al., 2009).**

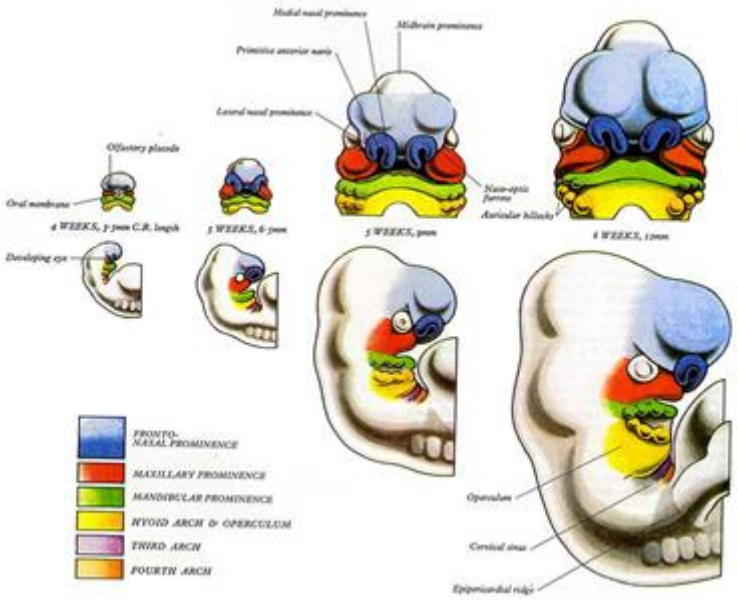

Fig 9. **A sequence of diagrams showing the superficial contributions of the facial prominences and pharyngeal elements to the development of the face (from 4th to 6th weeks) (Williams et al., 1989).**

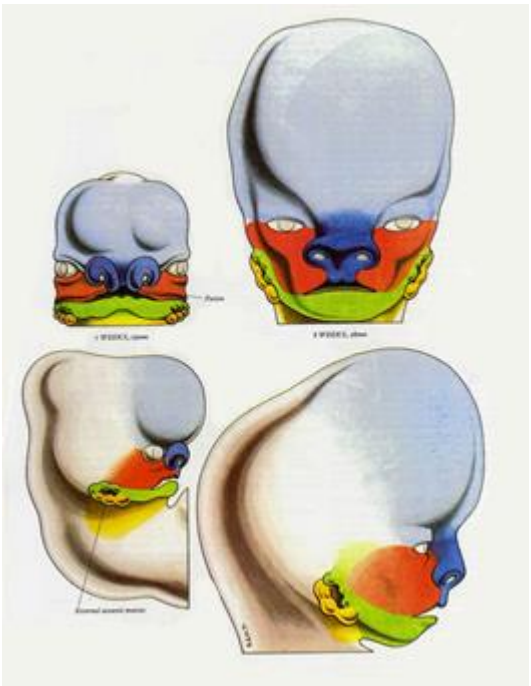

Fig 10. **A sequence of diagrams showing the superficial contributions of the facial prominences and pharyngeal elements to the development of the face (from 7th to 8th weeks) (Williams et al., 1989).**

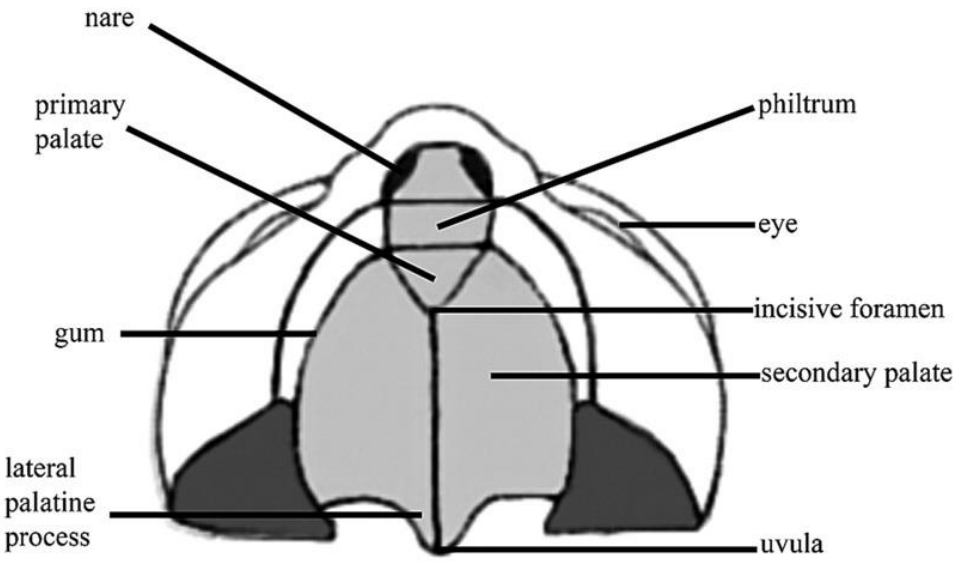

Fig 11. Draft of the primitive palate, incisive foramen, gum, lip and nose. Ventral illustration (Johnson et al., 2011).

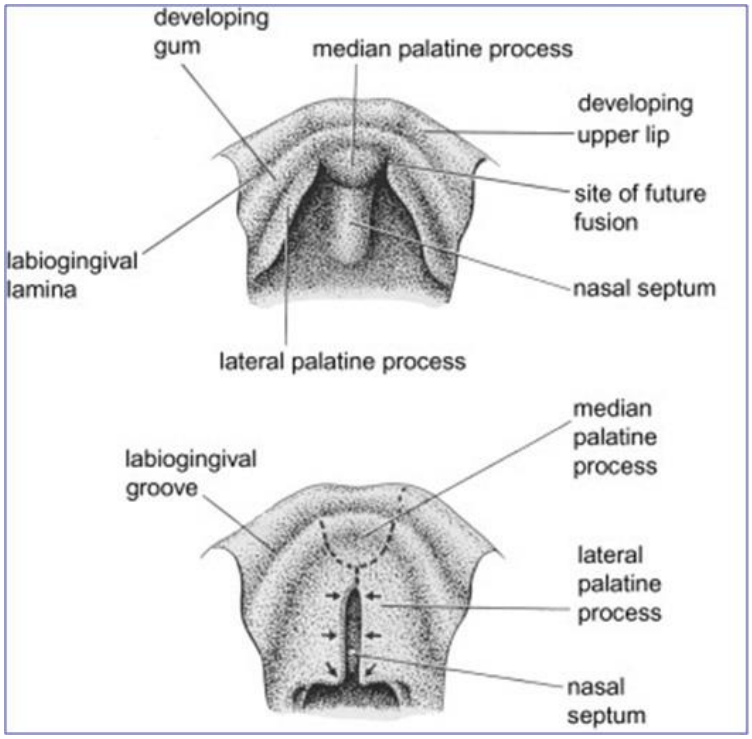

Fig 12. Development of the palate from 5th to 6th week (Moore, 1989).

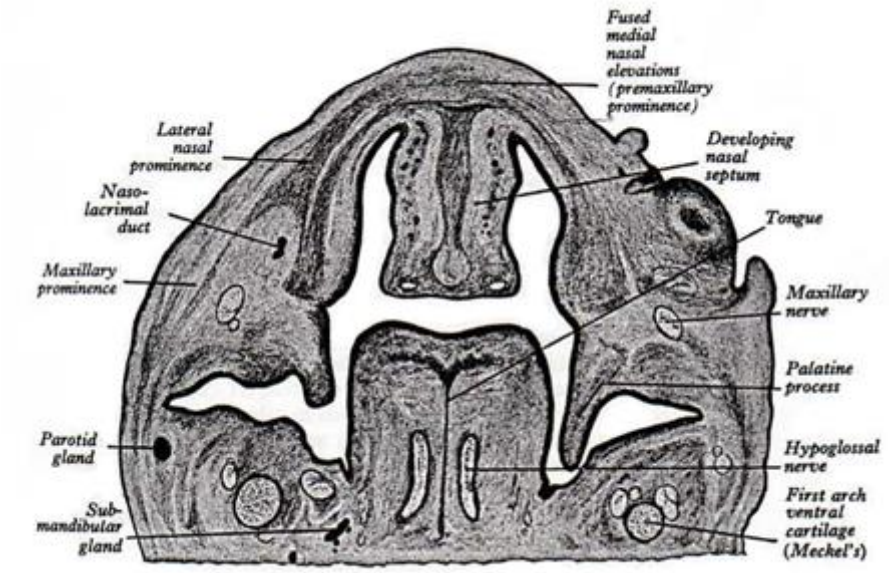

Fig 13. Oblique coronal section through the head of a human embryo 23 mm long. The nasal cavities communicate freely with the cavity of the mouth (Williams et al., 1989).

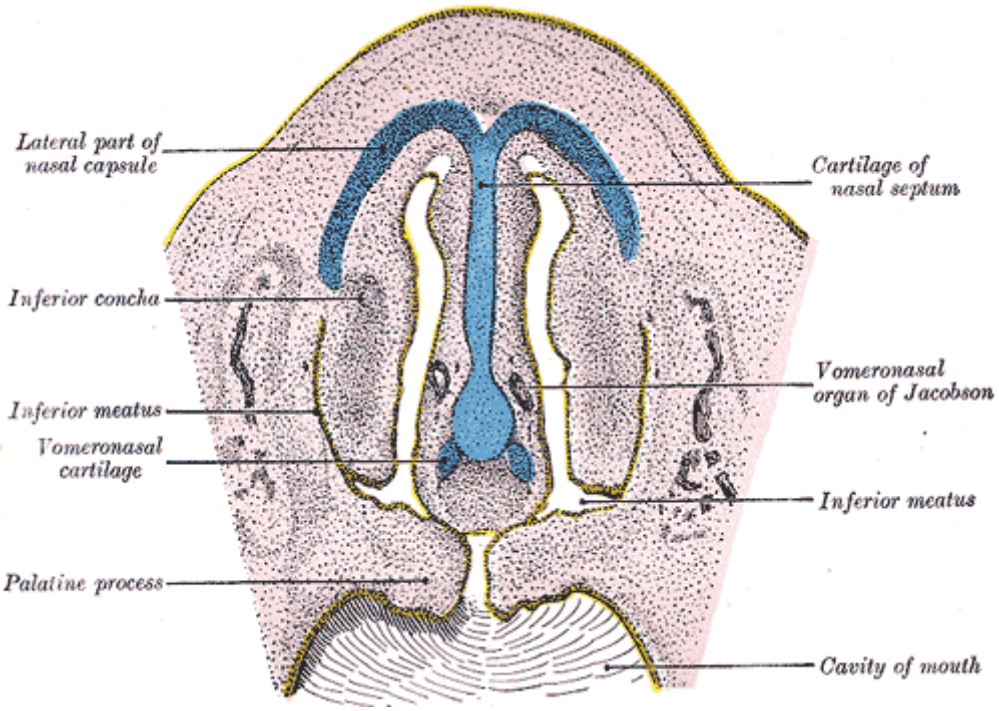

Fig 14. Coronal section through the nasal cavity of a human embryo 28 mm long. Region of fusion of the palatine processes (Gray, 1918).

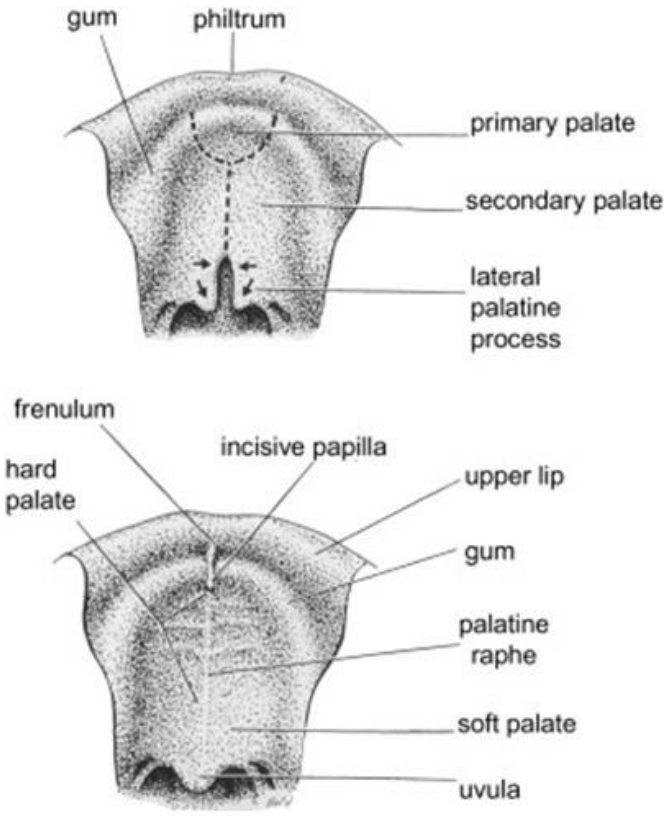

Fig 15. **Development of the palate: from 7th to 12th week (Moore, 1989).**

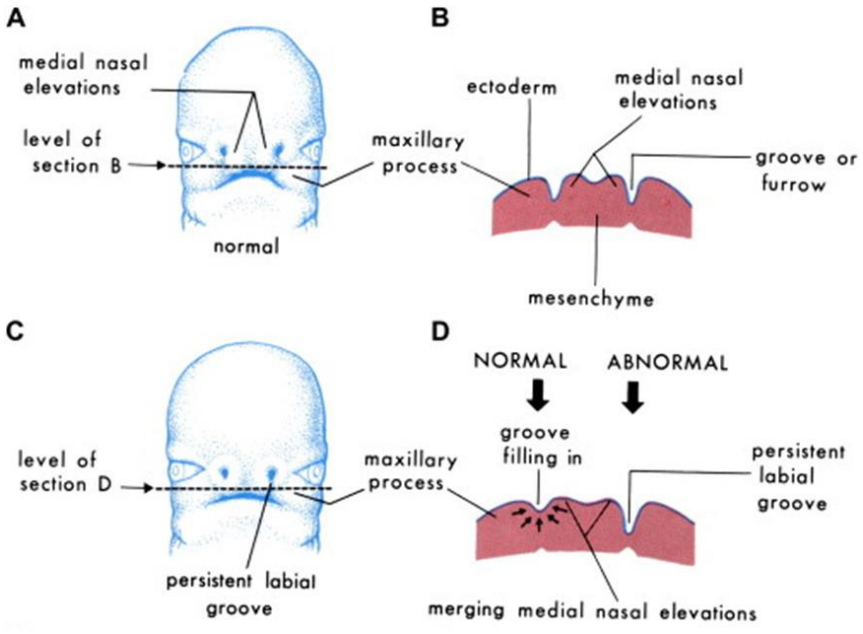

Fig 16. **Persistent fissure between the philtrum and the lateral part of the upper lip I (Moore, 1989).**

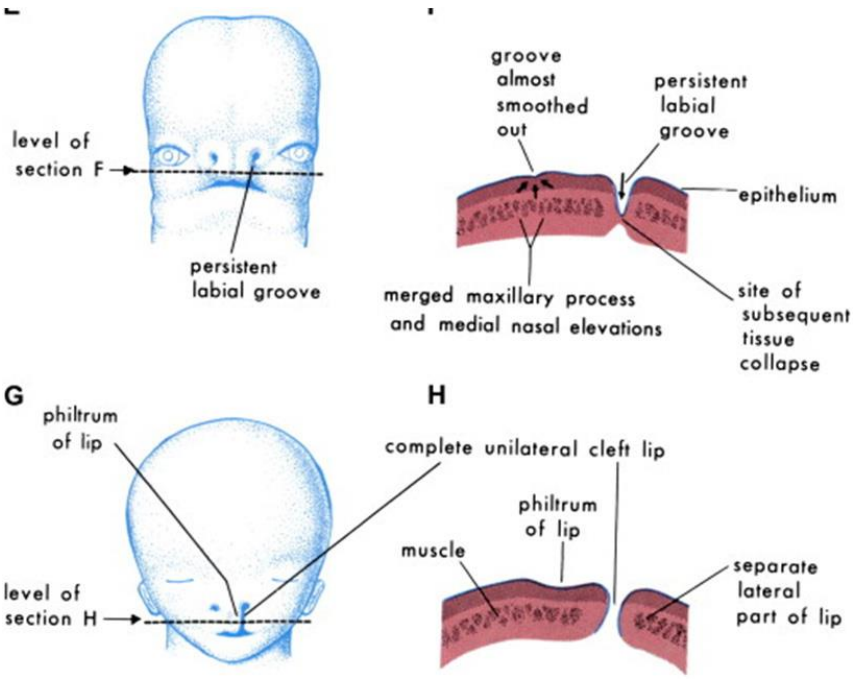

Fig 17. **Persistent fissure between the philtrum and the lateral part of the upper lip II (Moore, 1989).**

Fig 18. **Unilateral cleft lip and palate.**

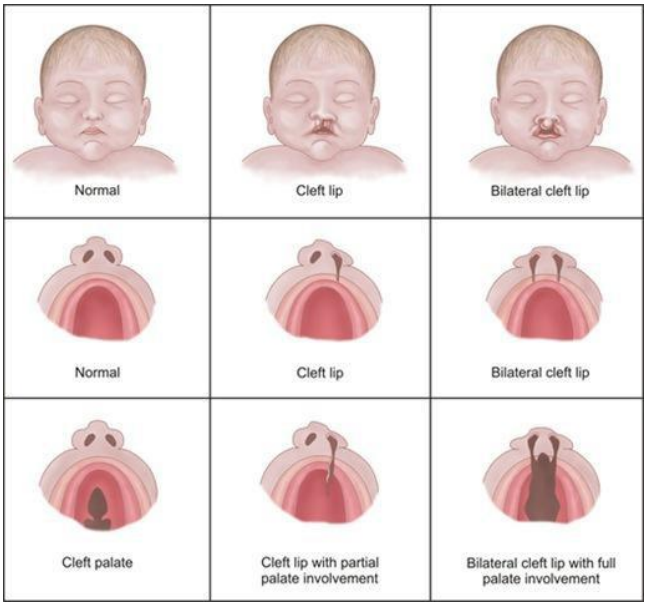

Fig 19. **Cleft lip and cleft palate: most common presentations. https://www.pinterest.com accessed on 14/12/2014.**

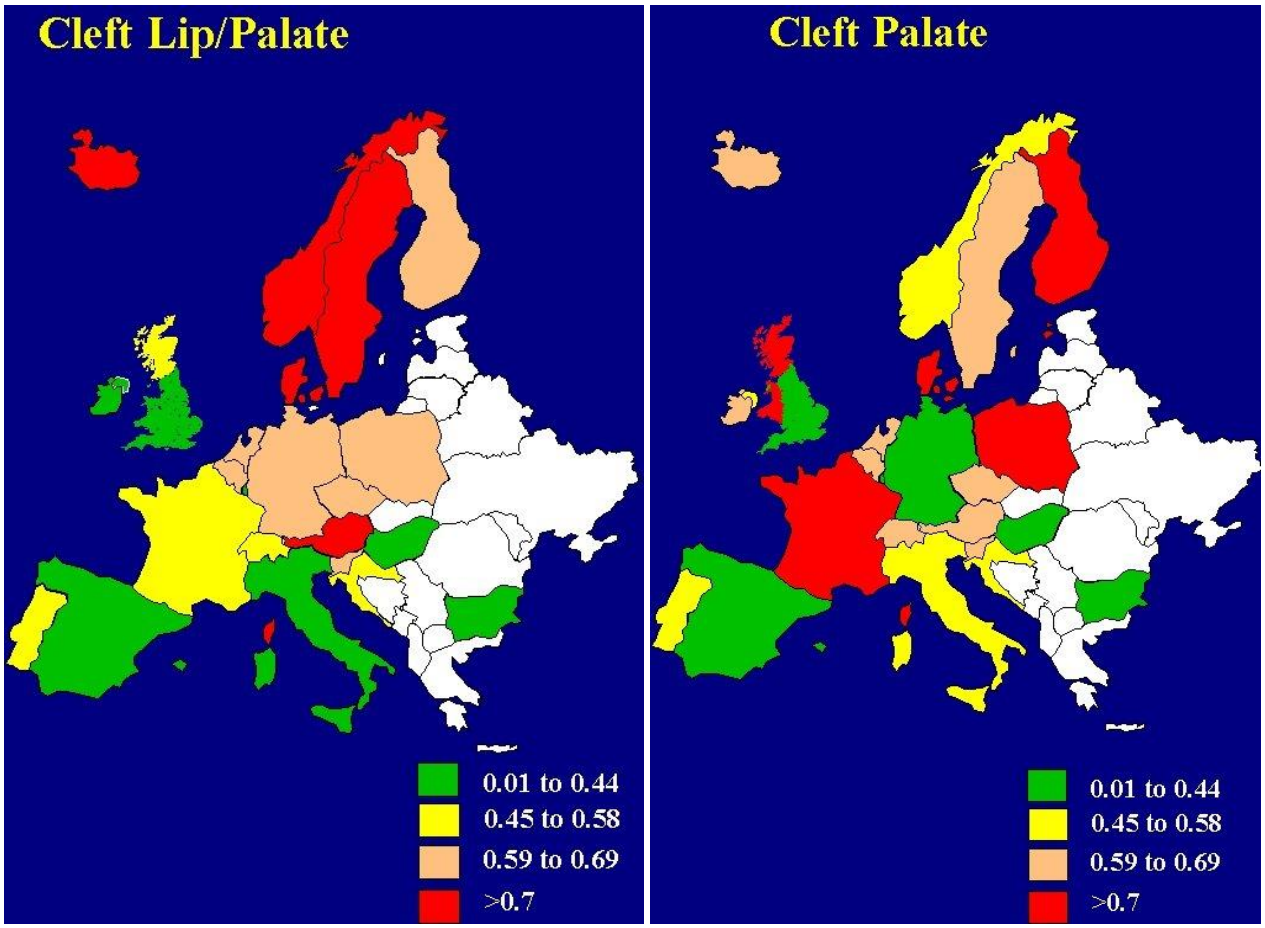

Fig 20. **European geographical distribution of cleft lip and palate and isolated cleft palate. http://www.eurocran.org/ accessed 14/12/2014.**

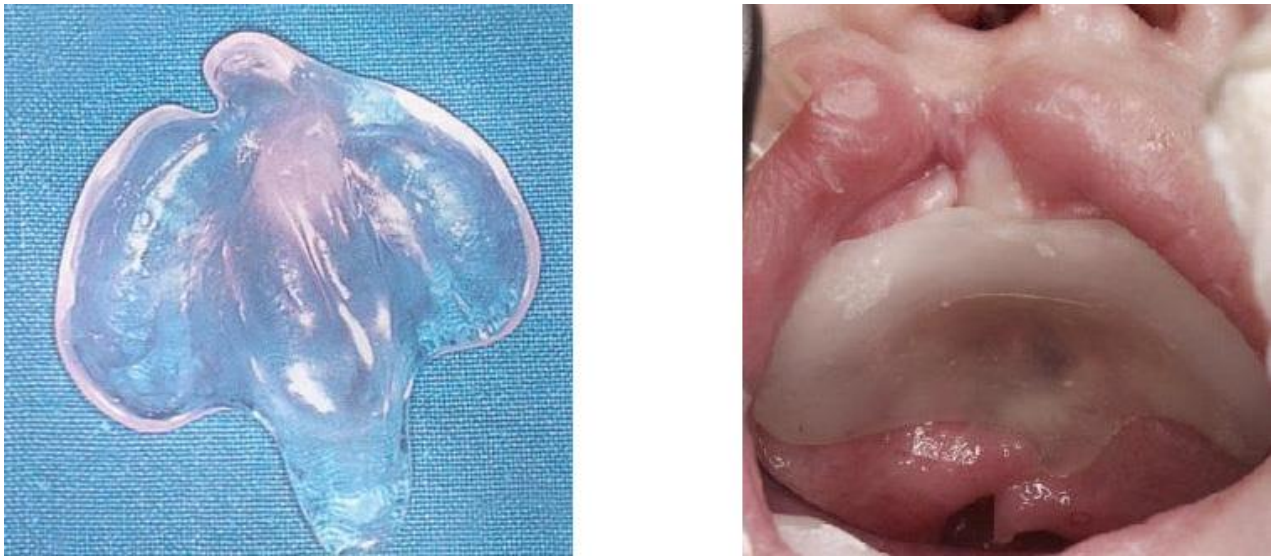

Fig 21. **Infant orthopedics: an acrylic plate.**

Fig 22. **Impression of a cleft maxilla (Gandolfini et al., 1993).**

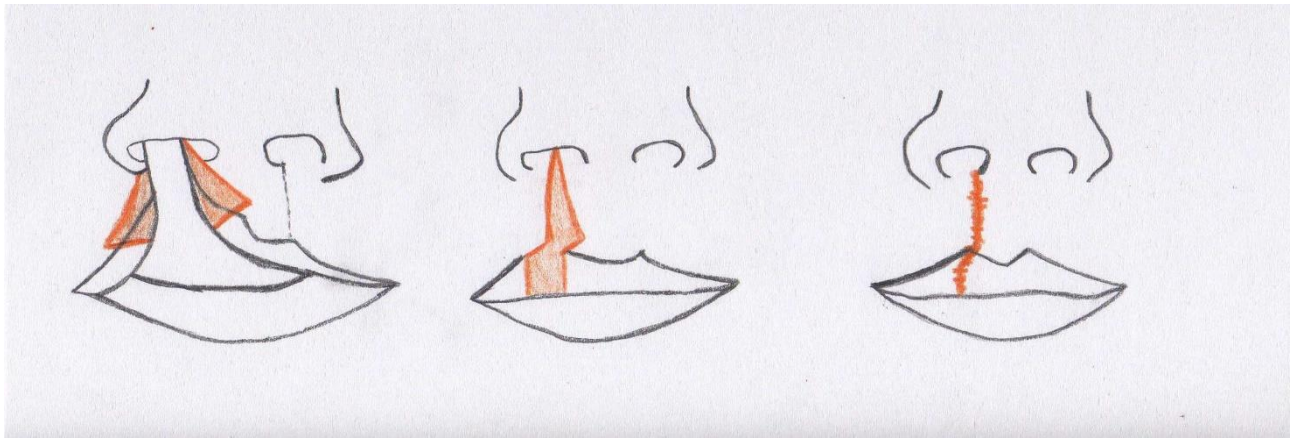

Fig 23. **Straight-line repair.**

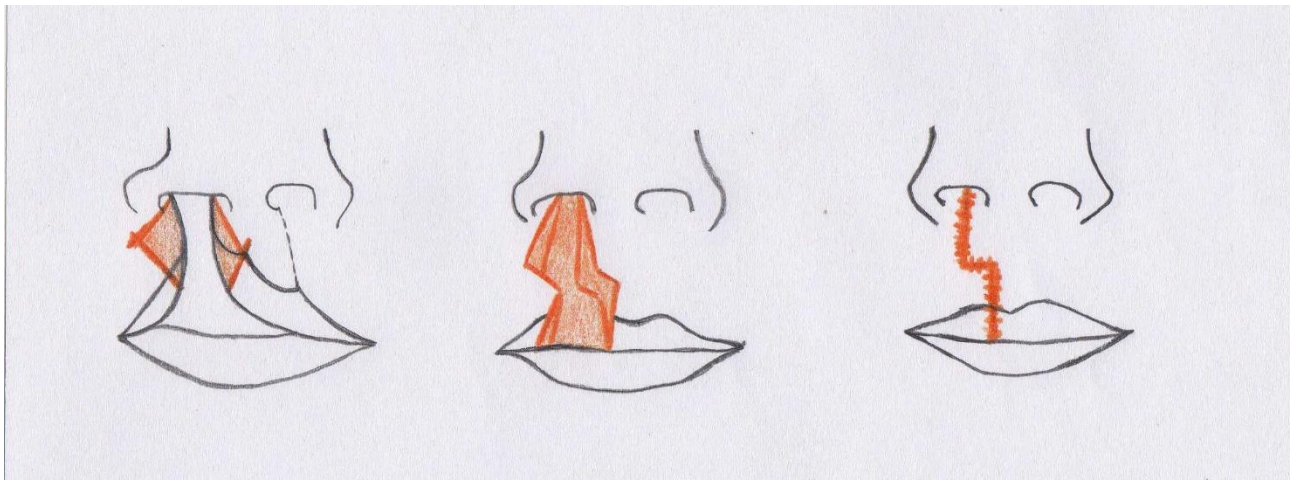

Fig 24. **Quadrangular flap according to Hagerdon and Le Mesurier.**

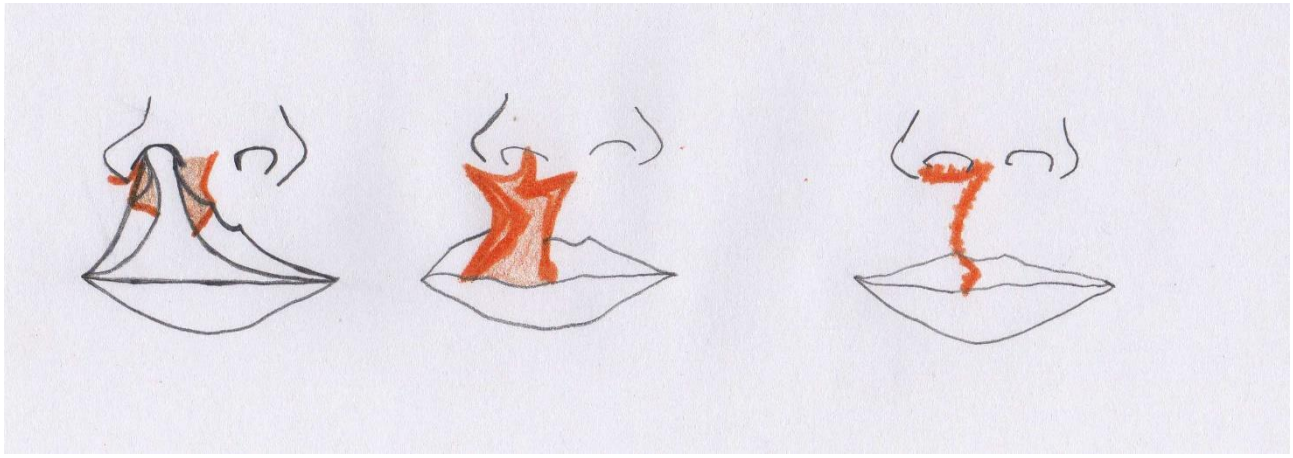

Fig 25. **Rotation advancement flap by Millard.**

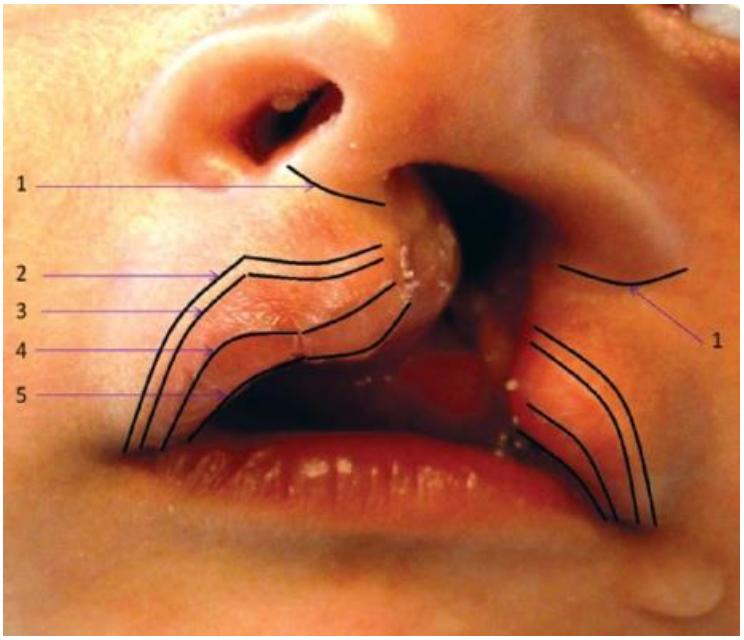

Fig 26. **Junctional lines of upper lip. Line 1: lip-columellar and lip-alar junction; line 2: junction between main zone and flat zone; line 3: vermilion-cutaneous junction (white line); line 4: junction between dry and transitional zones of the vermilion; line 5: vermilion-mucosal junction (red line) (Zayed et al., 2012).**

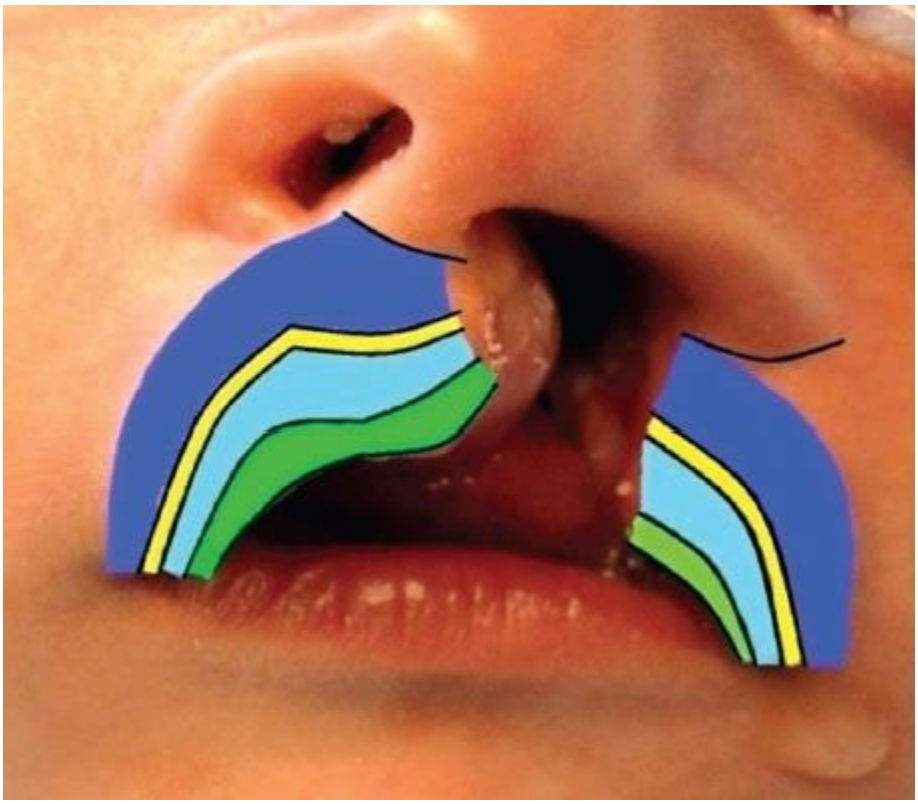

Fig 27. **Junctional zones of upper lip. Violet: main cutaneous zone; yellow: flat cutaneous zone; sky-blue: dry zone of the vermilion; green: transitional zone of the vermilion (Zayed et al., 2012).**

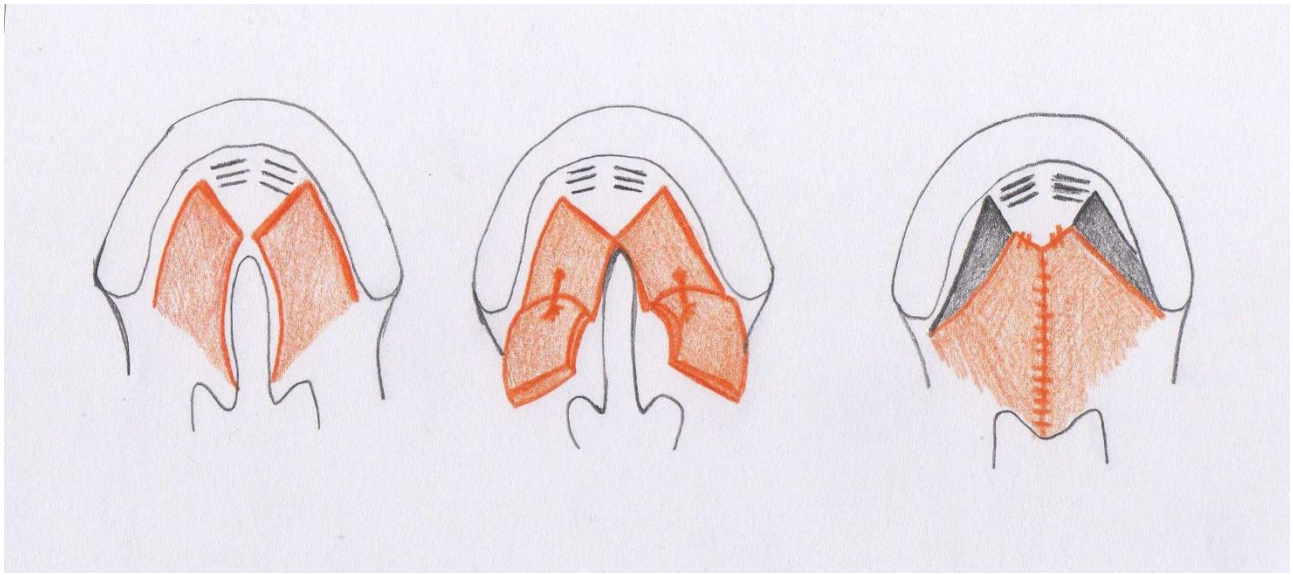

Fig 28. **"Push-back" technique by Veau Wardill Kilner.**

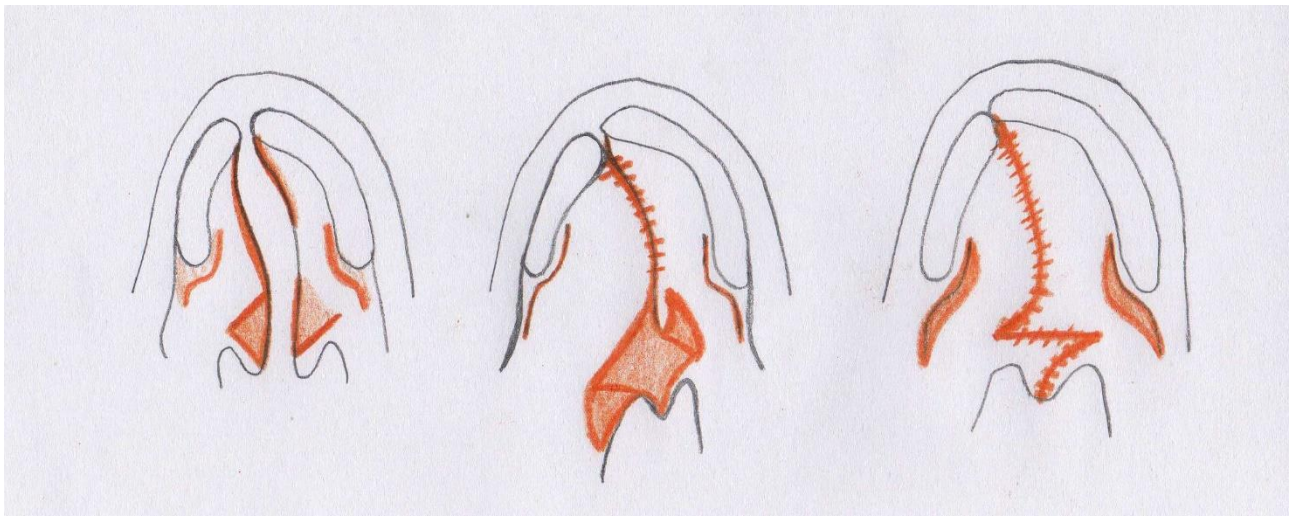

Fig 29. **Furlow double-opposing z-plasty.**

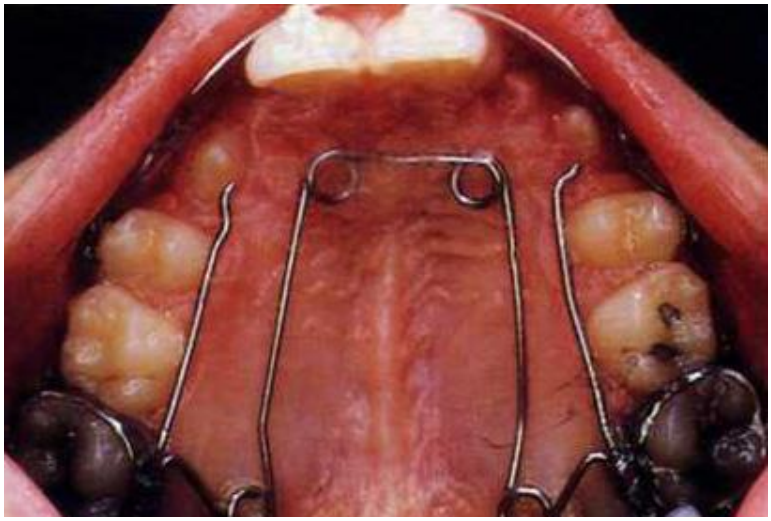

Fig 30. **Quad helix appliance in a case of bilateral cleft (Gandolfini et al., 1993).**

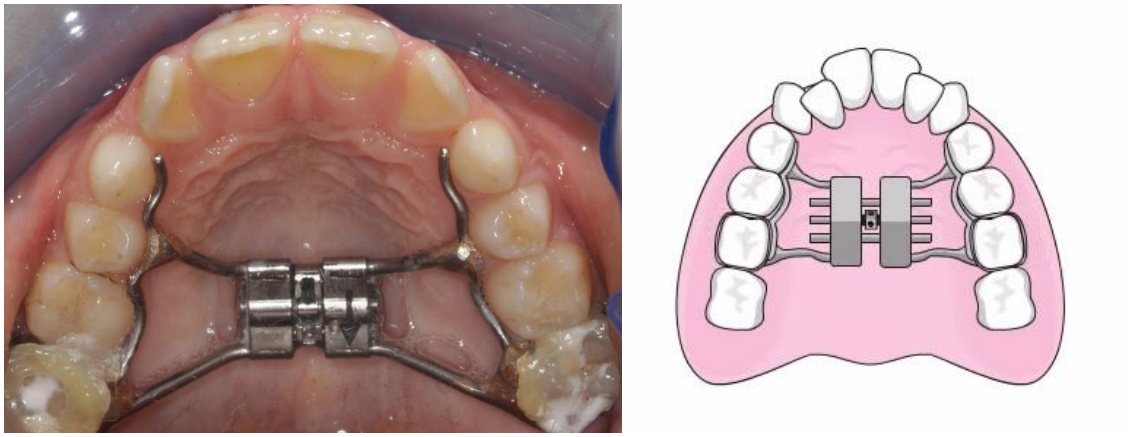

Fig 31. **Rapid palatal expander.**

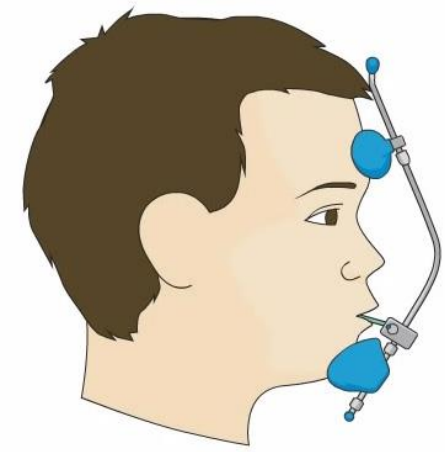

Fig 32. **Delaire face mask.**

Fig 33. **Orthodontic bracketing not involving the entire dentition.**

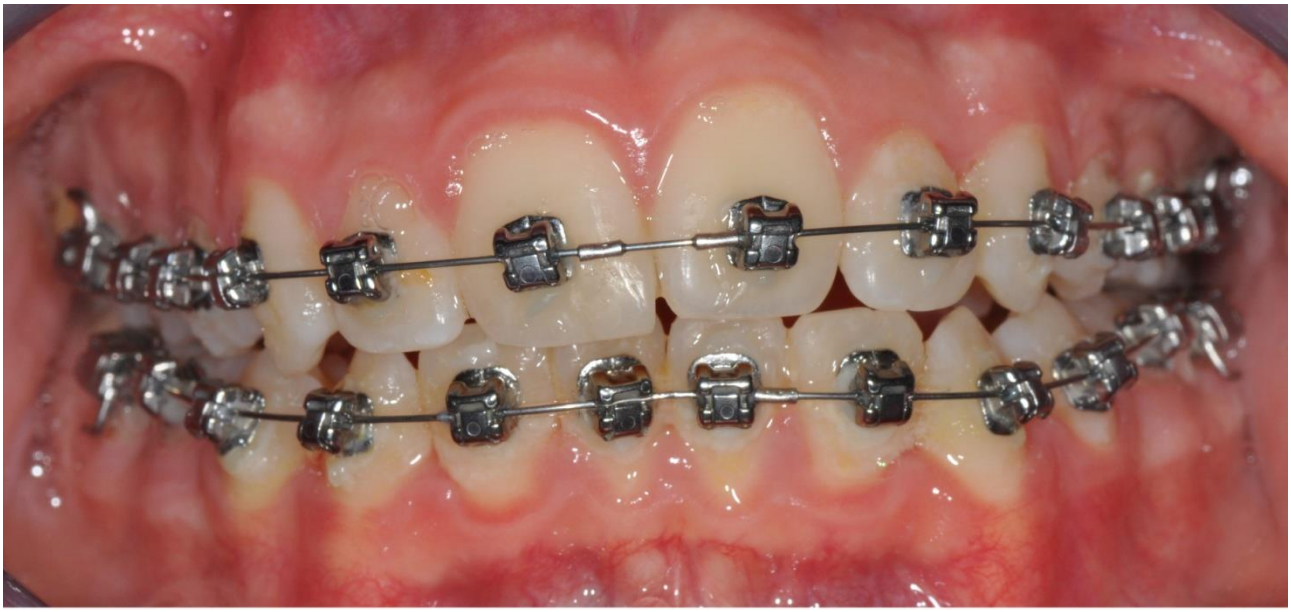

Fig 34. **Upper and lower arch bracketing.**

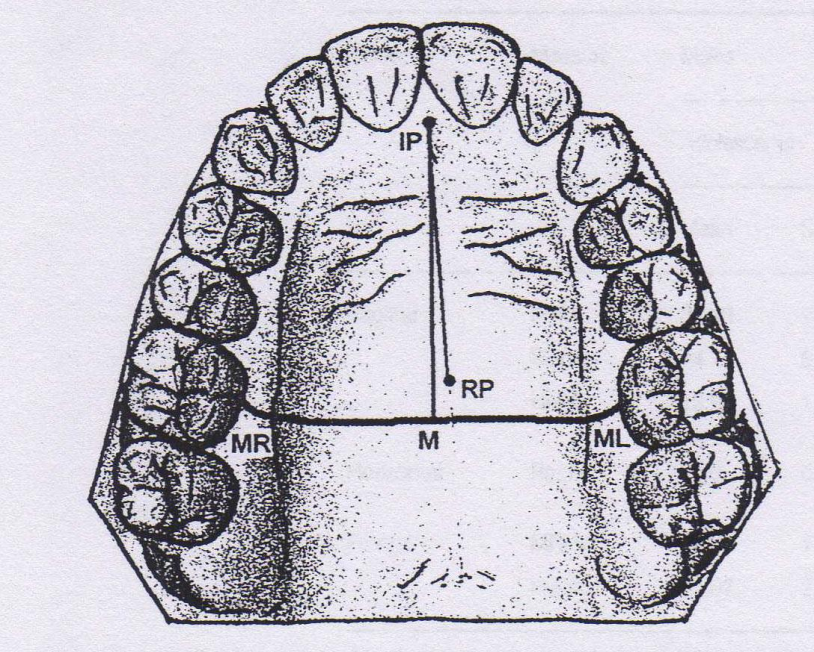

Fig 35. **Digitized points on the stone cast of each palate. IP: incisive papilla; RP: posterior-most raphe point; MR, ML: left and right molar points; M: sagittal molar point (Ferrario et al., 2001).**

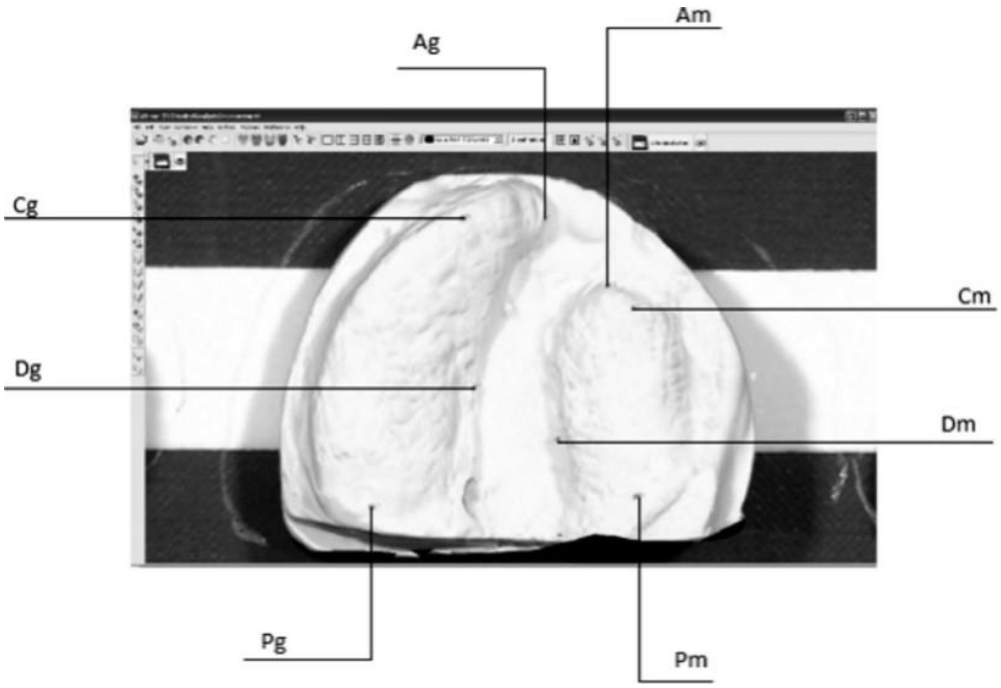

Fig. 36. **Landmarks identified both in the greater (g) and in the minor (m) segments. P = postgingivale; A = anterior alveolar; C = canine; D = deep cleft (Sforza et al., 2012).**

Tables

N.	Registries set	Rate x 10000	95% confidence interval	N. of cases
1	South Africa	4.76	3.28 – 6.69	33
2	Europe Mediterranean	8.80	8.22 – 9.41	856
3	USA East	10.02	9.16 – 10.93	500
4	United Arab Emirates	11.05	6.66 – 17.26	19
5	USA Atlanta	13.90	12.10 – 15.88	215
6	Italy – Sicily, ISAC	14.23	10.46 – 18.93	47
7	USA - Hawaii	14.35	11.29 – 17.99	75
8	Europe Central - East	14.91	14.32 – 15.51	2467
9	Europe British Islands	15.41	14.22 – 16.68	613
10	Cen-South America	16.16	14.88 – 17.52	587
11	Europe North	16.65	14.82 – 18.64	300
12	USA Central	16.82	15.87 – 17.81	1176
13	Australia Victoria	17.49	15.25 – 19.96	219
14	North America West	20.99	19.71 – 22.34	994
15	South America	21.68	19.91 – 24.74	220
16	North Europe	22.64	20.34 – 25.13	354
17	Japan	23.79	21.99 – 25.71	644

Table 1. Rates of typical oral clefts in 17 areas, observed by increasing rate (Mossey, 2007).

Gene	Gene expression pattern and craniofacial anomalies associated
PAX7	Expressed in craniofacial neural crest derivatives it causes malformation in the maxilla and nose in mice
ABCA4-ARHGAP29	Expressed in the medial and lateral nasal processes, maxilla, mandible and secondary palatal shelves
IRF6	Associated with shorter and rounded snouts and jaws
MSX1	Associated with anomalies of the frontal and nasal bone, reduced length of the mandible, abnormal dental development and cleft palate
FOXE1	Mutations cause Bamforth-Lazarous syndrome characterized by hypothyroidism, cleft palate and ocular hypertelorism
TGFB3	Associated with cleft palate
MAFB	Expressed in the craniofacial ectoderm, palatal shelves and nasal septum
LFFTY1	Expressed on the left side of the floor palate and acts as the anterior midline barrier to signals that determine leftness
LFFTY2	Mutations cause left isomerism (both sides develop left side characteristics)
PITX2	Expressed in the epithelium of maxilla, mandible and dental lamina. Mutations cause cleft palate and arrested tooth development
ISL1	Contributes to both cardiac and head muscle progenitors and therefore controls facial expression and masticatory muscles
SNAI1	Mutations cause fusion failure and multiple craniofacial defects including failure of the mandible to move forward similarly to Pierre Robin sequences
SATB2	Associated with isolated cleft palate

Table 2. **Listing and description of clefting and craniofacial candidate genes (Miller et al., 2014).**

2- Material and Methods

2.1- Subjects

A total of 96 palatal cast models, obtained from 32 neonatal patients (15 girls and 17 boys) with unilateral cleft lip palate (UCLP), attending the Fundacion Clinica Noel de Medellin (Colombia) were collected and sent to our Laboratory in Milan, where the casts were digitized.

These palatal casts were collected during a clinical study performed to evaluate the 3D morphological effects of various treatments on the growing segments of dental arches of patients younger than 1 year of age and not subjected to early surgical procedures or prior orthopedic treatments. The impressions were taken at the three different times during follow-up (fig 37-40):

-prior to presurgical orthopedic treatment (mean age 10.5 days; SD 4.8)

-before cheiloplasty (mean age 83.3 days; SD 6.6)

-after cheiloplasty (mean age 317.1 days; SD 44.2).

Presurgical orthopedic treatment was performed with either passive (10 boys and 6 girls) or active plates (7 boys and 9 girls). All subsequent measurements were made blindly to the kind of used plate. While the passive plates (Hotz's plate) are made of hard acrylic and are not adjusted over time, the active plates (PNAM – presurgical nasoalveolar molding) have an intraoral side covered with soft acrylic and are adjusted on a weekly basis to perform trimming of the intraoral and nasal portion of the appliance or to add acrylic as needed (Lopez-Palacio et al., 2012).

2.2- Instrumentation

We used a 3D stereophotogrammetric system (Vectra 3D; Canfield Scientific, Inc., Fairfield, NJ, USA) to digitize the palatal casts and then the stereophotogrammetric softwares to analize our files. The stereophotogrammetric method consists of a group of cameras with a fast capture time; the cameras capture different images of the subject from multiple angles simultaneously, and a dedicated software reconstructs a digital 3D image

Several systems using 3D stereophotogrammetry are available on the market. We used the Vectra 3D Imaging System (fig 41). It is a modular 3D image-capturing system designed to capture and process stereo images. The system consists of 2 pods, including 3 cameras (2 black and white and 1 color) and a projector in each pod. Basically, the method of active stereophotogrammetry is used: a fine pattern is projected onto the facial surface or onto various objects (i.e. dental casts), thus magnifying the differences between facial areas of various depth. Subsequently, synchronized 2-

dimensional images of the subjects are captured within 0.75 millisecond. By using a dedicated software, the information is used to work out the 3D reconstructions that subsequently can be processed, analyzed, manipulated, and measured. A calibration step is required daily and before patient arrival or anytime the system has been moved. Its accuracy has already been verified (de Menezes et al., 2010).

2.3- Data collection and landmarks

Before the digitization, several landmarks were marked on each palatal cast (fig 40). The anatomical reference landmarks assessed the two cleft segments separately. Landmarks were identified according to the previous investigation by Sforza et al. (2012).

The palatal casts were then digitized (fig 42) and the appropriate files were analyzed using the stereophotogrammetric software.

2.3.1- Repeatability

The base of each greater and minor cleft segment was identified by outlining it with a series of landmarks. They were placed at the border between the alveolar process and the maxillary bone; the process was made starting from the deepest point of the alveolar process (palatal surface).

20-30 landmarks were then marked on each segment with a nearly equidistant position and following the border in a clockwise direction (fig 43).

A subset of 30 casts was randomly selected from the complete set of 96 casts, and used for method error.

Different operators and the same operator over time calculated the area included by the landmarks to evaluate method repeatability.

2.3.2- Areas

After verifying data repeatability, the area of each alveolar segment was obtained.

The process was helped by the visualization tool of the stereophotogrammetric software (fig 44, 45) that shows only the outline of the image (Mirror imaging software, Canfield Scientific, Inc., Fairfield, NJ, USA). The measurement protocol is detailed in appendix 1.

2.3.3- Volumes

Afterwards we also devised a new method to determine the volumes of the greater and minor segments of the cast. We used the “Paint” program to create a two-dimensional, monochromatic plane surface, that was imported in the image of the cast where we needed to obtain the volume.

In every cast the area of either the greater or the minor segment was previously selected. The landmarks outlining the borders of the area were projected on the two-dimensional surface.

A tool of the Vectra System was used to superimpose the corresponding landmarks. With this method we obtained the volume of the segments we were analyzing and subsequently the volumes enclosed by the two surfaces were calculated (fig 46-49). The measurement protocol is detailed in appendix 2.

2.4- Analysis of dental cast measurement

The accuracy and repeatability of the 3D stereophotogrammetric system had been previously studied (de Menezes et al., 2010).

In particular, to evaluate the reproducibility of the operators’ tracings, that is the repeatability of our method, we decided to verify the measurements of the areas calculated by two different operators and the same operator over time by using the Paired Student’s t-test (systematic error).

Additionally, the technical error of measurement (TEM) was used to evaluate the random error. The TEM or Dahlberg’s error is calculated as:

$$TEM = \sqrt{\sum \frac{D}{2n}^2}$$

Where D is the difference between each pair of replicate measurements and n is the number of pairs. The percentage ratio between the squared TEM and the global variance was also computed to verify the actual amount of sample variance due to the method error.

Descriptive statistics were obtained for each segment, time point and kind of plate.

Area and volume measurements were compared with a three-factor repeated measures analysis of variance (ANOVA) to determine the differences between plates (active and passive; between subject factor), alveolar segments (minor and greater; within subject factor), and time (A, B, C; within subject factor). Post-hoc tests were made where appropriate. Box’s Test of Equality of Covariance Matrice and Levene’s Test of Equality of Error Variances found that the homoscedasticy hypothesis was verified in all occasions.

Additionally, for both alveolar area and volume, the percentage of growth between consecutive time points was computed separately for the two alveolar segments as:

After orthopedics: (value at time point B – value at time point A) / (value at time point B) x 100

After cheiloplasty: (value at time point C – value at time point B) / (value at time point C) x 100

Descriptive statistics were calculated for all growth percentages to obtain a general information about the time-related intra-individual variations.

For all analyses, a p-value of 0.05 was used to assess statistical significance.

3- Results

3.1- Repeatability and reliability

Tables 3 and 4 report the descriptive statistics for operator's errors obtained on the alveolar arch for area measurements.

No systematic errors between measurements obtained in two different occasions by the same operator (S1-S2) and between different operators (O1-O2) were found ($p>0.05$) indicating that the method had no bias. Low TEM values correspond to more repeatable measurements: the random error was lower than 0.32 cm^2. Overall, the method error was less than 5% of the total variance for inter-operator assessments and less than 2% for intra-operator assessments.

3.2- Areas

The complete sample of area measurements divided by type of plate is reported in table 5. Statistics for palatal segment area in the three analyzed time points are reported in table 6.

Highly significant effects of alveolar segment and time were observed (three-factor repeated measures analysis of variance, $p<0.0001$, table 7). Post hoc tests found significant differences at all time points. Instead no differences were found for the kind of plate. There was also a significant interaction between time and segment, showing that the minor and greater segments grow differently through the time, independently of the type of used plate (all the interactions including the plate factor were not significant).

Figure 50 shows the percentage growth of alveolar area between consecutive time points. Considering that the kind of plate had no effect on palatal area, all palates were analyzed together. On average, growth was somewhat larger in the minor segment and in the first interval, just before surgical treatment.

3.3- Volumes

The original sample is reported in table 9. Statistics for palatal segment volume in the three analyzed time points are reported in Table 10.

Highly significant effects of alveolar segment and time were observed (three-factor repeated measures analysis of variance, time $p = 0.0003$ and segment $p<0.0001$, table 11). Post hoc tests

found significant differences between the first and third, and the second and third time points. No differences were found for the kind of plate. Conversely, there was no interaction between time and segment as we found for area analysis and no interaction between time and plate.

Figure 51 shows the percentage growth of alveolar volume between consecutive time points. All palates were analyzed together. For both segments, an increase in volume was noticeable only after surgical treatment; indeed, for both time intervals, large intra-individual variations were found.

4- Discussion

The treatment of children with UCLP requires collaboration among multiple specialists and it is associated with variable outcomes related to patient's characteristics and surgical technique used.

There is a need for an internationally agreed objective method of assessing cleft related deformities to compare the results of planned treatments. The problem that occurs is the need for standardized data. Mosmuller et al. (2013) made a review of literature from June 2003 to July 2011 yielding 428 articles comparing different methods of scoring systems (anthropometric measurements, 2D and 3D imaging photographs) in cleft related facial deformities.

Additionally, Kasaven et al. (2013) determined the accuracy of volumetric measurements of alveolar bone defects using cone-beam computed tomography (CBCT) scans. The use of CBCT should be limited to selected patients and it cannot be proposed for longitudinal assessments.

Most cleft centers rely on conventional two-dimensional photography for longitudinal documentation of facial form during the treatment of cleft lip and palate. Although convenient, the outcome analysis using two-dimensional images are prone to errors, secondary to variations in camera angle (error from parallax). Originally direct anthropometric analysis of facial form was used, but this method is time-consuming and difficult to perform on awake infants younger than 1 year (Tse et al., 2014).

Although there is a wide variety in study design, the 3D imaging seems most reliable in assessing cleft related facial deformities and gradually it is becoming more affordable replacing classical methods to quantify surface topography (Sforza et al., 2012).

Digital 3D stereophotogrammetry seems to be the ideal method of capturing three-dimensional facial form in multiple orientations directly from the patients or from their palatal casts. The reliability of anthropometric measurements by using the digital three-dimensional stereophotogrammetry has already been evaluated on mannequin heads (Weinberg et al., 2006), on normal adults (de Menezes et al., 2010; Weinberg et al., 2004; Wong et al., 2008), on dental cast (Sforza et al., 2012) and on children and adults with non-cleft facial dysmorphology (Aldridge et al., 2005; Heike et al., 2009). A quick image acquisition reduces the effects of subject movements; in addition, there is no need for direct contact with the facial surface, thereby avoiding modification of soft tissues, which may cause errors in direct measurements (Simanka et al., 2011). Of course, movement and deformation are not of concern for dental casts.

Since craniofacial structures, in particular in syndromes like cleft palate, are very complex to examine, the 3D images have several advantages including accurate measurements, storage, rapid image capture (scan time 0.3 ms) and non-invasive nature (Proff et al., 2006; Sforza et al., 2013). Furthermore they can grant information exchange with different centers for planning medical procedures and treatments (Mello et al., 2013).

Data obtained can be used to assess the 3D changes occurring in the maxillary arch of unilateral cleft lip and palate patients with the use of active or passive presurgical orthopedic plates.

Most previous studies investigated the longitudinal modifications of palatal distances only, assessing the various growth patterns of the greater and the minor segments (Rousseau et al., 2013; Sabarinath et al., 2010). These assessments can provide useful information for a better treatment and children follow-up, but they are relative to single optical planes. To overcome this limitation, palatal areas and volumes can be measured, thus offering a more comprehensive evaluation, that considers also the effect of the various surgical and orthopedic techniques (Berkowitz et al., 2005).

These measurements are more complex than simple linear distances, and the relevant protocols may involve a larger number of steps, and therefore be more prone to error (Sforza et al., 2012). Thus, we devised a new system for area and volume identification and quantification. After the evaluation of the reliability and repeatability in identifying and measuring the area of alveolar segments, we analyzed areas and volumes of the greater and minor segments and how they changed during the first year of age. Instead reliability and repeatability were not evaluated for volume measurements since they are directly obtained starting from the previous area values.

Significant differences were observed for the alveolar segment (minor and grater), time (prior to presurgical orthopedic treatment, before cheiloplasty and after cheiloplasty) both in area and volume measurements. Additionally, the interaction between alveolar segment and time was significant for area measurements.

For the alveolar segment, the congenital cleft divided the alveolar arch in greater and minor segments and both segments increased in length, area and volume in all patients, irrespective of the kind (active or passive) of plate. We suppose that the maxillary segments have self-determining growth or have the potential to respond to the growth guidance provided by the appliance during the neonatal period. This is in accordance with Grabowski et al. (2006) who suggest that the combination of presurgical orthopedic treatment in infants stimulates the growth and harmonizes the function with minimally invasive cleft surgery.

Analyzing the three different time points, a highly significant difference was detected ($p<0.0001$ for areas and 0.0003 for volumes). This effect was expected not only for the physiological growth of the children, but also for the treatment received during each time interval. The children at time A (prior to presurgical orthopedic treatment) were in their first two weeks of life, they had nearly 3 months at time B (before cheiloplasty) and 10.5 months at time C (after cheiloplasty). Furthermore the treatment received in each time could stimulate arch growth. Accordingly to Grabowski et al. (2006), all procedures taken in cleft patients aim at promoting physiological patterns of function and the bone growth can be stimulated in the first year of life only.

The statistical significance found for the interaction between alveolar segment and time in area measurements shows that the potential growth of the minor segment was larger than that of the greater one. A positive effect of treatment may be claimed. Baek and Son (2006) found that the growth of greater segment was restrained by the presurgical molding treatment, but it resumed

after cheiloplasty. These findings differ from Berkowitz et al. (2005), who described that right and left lateral palatal segments, whether large or small, grew at the same rate, independent of any presurgical treatment or the timing of surgery when compared with control series (no clefts in the hard palate). The lack of significant segment x time interactions in volume measurements seems in accord with Berkowitz et al (2005).

After cheiloplasty (time interval B-C), the areas of both alveolar segments had similar percentage progresses (on average 7.9% greater segment, 9.2% minor segment). This outcome is in accordance with Eichhorn et al. (2011), who found that additional dental casts obtained in single cases at later surgical procedures prove a rapid initial reduction of alveolar cleft width followed by a reduced velocity of movement. Additionally, the same authors reported that, after lip closure, the growth of the arch depth and the intercanine width was significantly reduced showing an immediate effect of lip closure on maxillary arch shape. In the period between lip closure and palatal closure the growth of the palatal arches changed into direction of the non-cleft controls while the growth velocity of the intercanine width of the anterior arch remained lower than that measured in the non-cleft controls (Heidbuchel et al., 1998).

In contrast, volume variations between time points A and B were minimal for both the greater and the minor segments (on average 0.88% for the minor segment and 0.71% for the greater segment), whereas they increased after cheloiloplasty (9.52% for the greater segment and 6.60% for the minor segment). Indeed, when analyzing single patients, a large intra-individual variation was observed, and the current calculation can give only a general information about the mean growth patterns. Apparently, pre-surgical orthopedics modified segment shape without volume changes, while surgical treatment had a major and more global effect on palatal dimensions. The use of a 3D optical scanner provided us a set of more comprehensive values to assess the actual effect of combined treatments of cleft palate children.

No significant effect of the kind of plate was observed; more investigation is needed on this topic. Indeed, literature reports unclear results about the possible different influence of a variety of plates (Berkowitz et al., 2005; Lopez-Palacio et al., 2012; Papadopoulos et al., 2012).

Our study limitations were represented by the reduced follow up period of the study; in fact, we collected only three measurements from each patient during their first 12 months of life, whereas it is known that cleft lip and palate patients will have to undergo several surgical treatments along their life to obtain a better aspect of their face together with a sound functionality (Berkowitz et al., 2005). Furthermore, it has been suggested that a more detailed assessment of the time-related modifications occurring during the first year of life may help in better understanding the growth potentials of cleft palate children and their response to treatment (Berkowitz et al., 2005). Nonetheless, the procedure for palatal impression is complex for babies, and we believe that additional, intermediate time points may reduce family compliance and increase possible adverse side effects. The current three time points seem to represent a good compromise between benefits and risks.

However reaching the anatomical and functional maxillofacial integrity is just one of the surgical goals of cleft repair. Another limitation of the study is that the 3D stereophotogrammetry investigative approach of the alveolar segments can give benefit in evaluating the effects of different treatment protocols on bone and dental arches, but it cannot allow assessments of the facial soft tissues. Beauty and symmetry of the face are important elements in human relationship and the achievement of a pleasant face is still a tough challenge (Gesch et al., 2006; Russell et al., 2009).

5- Conclusion

In our study we showed that the alveolar bone delimitation on digital dental casts, area and volume measurements, recorded by a 3D stereophotogrammetric system is repeatable and reliable for assessing stone casts of patients with UCLP during the first year of age.

This procedure can be used to monitor longitudinally the evolution of orthopedic healing through non-invasive acquisition of dental casts and facial morphology thus guiding clinicians in real time analyses for maxillo-facial surgery.

The lack of dangerous procedures on young patients is a further benefit given by the 3D stereophotogrammetric system.

The follow up for the period of treatment using presurgical orthopedics showed a reduction in alveolar cleft width and lip width relative to facial growth, making subsequent surgery easier.

Those therapies indicate that maxillary segments have the potential to respond to presurgical orthopedic treatment during the early neonatal period, while early palatoplasty of soft palate at 12 months of age and hard palate at 18 months of age have a considerable benefit for the palatal development of patients with complete unilateral cleft lip and palate (Yamanishi et al., 2009).

Future investigations should expand the number of analyzed patients and 3D stereophotogrammetric system may make it easier introducing data exchange and promoting close cooperation among various cleft centers of treatment of these complex facial deformities.

Other studies are necessary to evaluate more complex palatal measurements and structural information on surface areas and volumes and curvature starting from the images recorded by the 3D stereophotogrammetric system.

Appendix 1

The area measurement protocol consists of the following steps:

1- Open the file of the digitized cast (fig 41).

2- Mark from 20 to 30 landmarks surrounding the base of the greater or minor cleft segments, starting from the deepest point of the alveolar process.

3- Progress in a clockwise direction until all the alveolar process is outlined (fig 42).

4- Use the tool of the stereophotogrammetric software that shows only the outline of the image (show outline only) to obtain the correct position of the landmarks (fig 43).

5- Use the tool of the stereophotogrammetric system to calculate the area (fig 44) enclosed by the landmarks (Landmark ----> Select all; Area ----> Select ----> Extend using landmarks; Measure ----> area of selection).

Appendix 2

The volume measurement protocol consists of the following steps:

1- Open the file of a digitized cast and select all the landmarks (Landmark ----> Select all) and the previously calculated area (Area ----> Select ----> Extend using landmarks).

2- Create a two-dimensional monochromatic plane surface with “Paint” computer program and import it (fig 45) with the dental cast (Open image as a flat surface).

3- Project the landmarks outlining the border of the area on the two-dimensional plane (Landmark ----> Select all; Landmark ----> Project selected landmarks) so that every point had its corresponding one on the virtual plane (fig 46).

4- Superimpose the two surfaces by using the landmarks with the same number (Surface ----> Register surface ----> Landmarks with corresponding names). In this way the virtual plane will cut the cast at the base of the alveolar process (fig 47).

5- Use the tool of the stereophotogrammetric system to calculate the volume between two objects. The software will calculate only the volume of the alveolar process over the cutting plane (fig 48) (Measure ----> Volume ----> Between two surfaces).

Figures

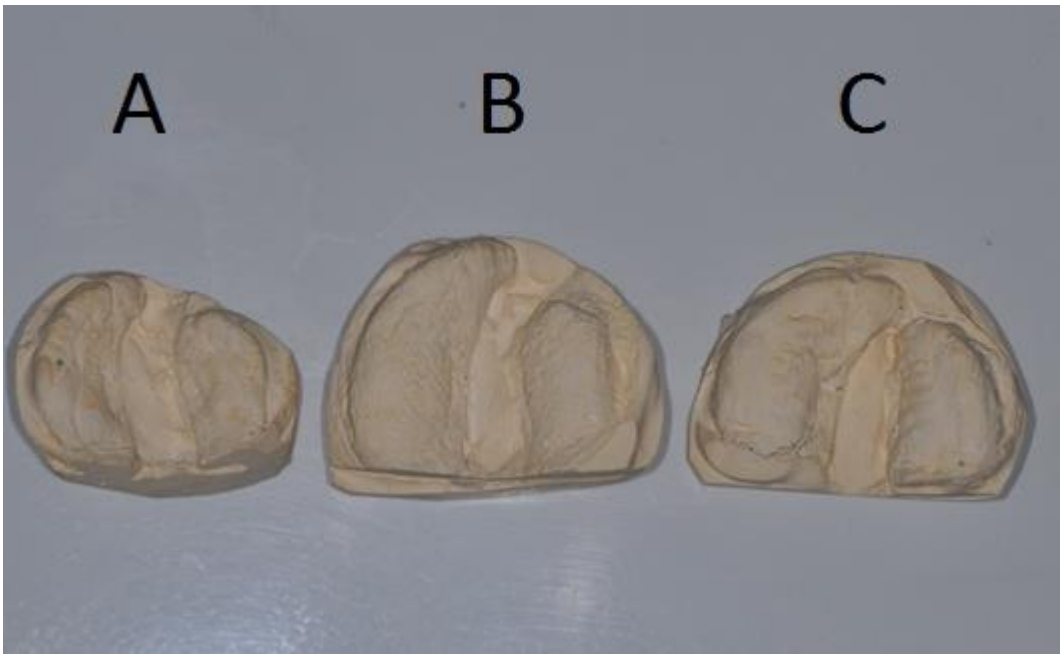

Fig 37. **Dental casts of the same patient at the three different time points: from left to right, before presurgical orthopedics (A), before cheiloplasty (B) and after cheiloplasty (C).**

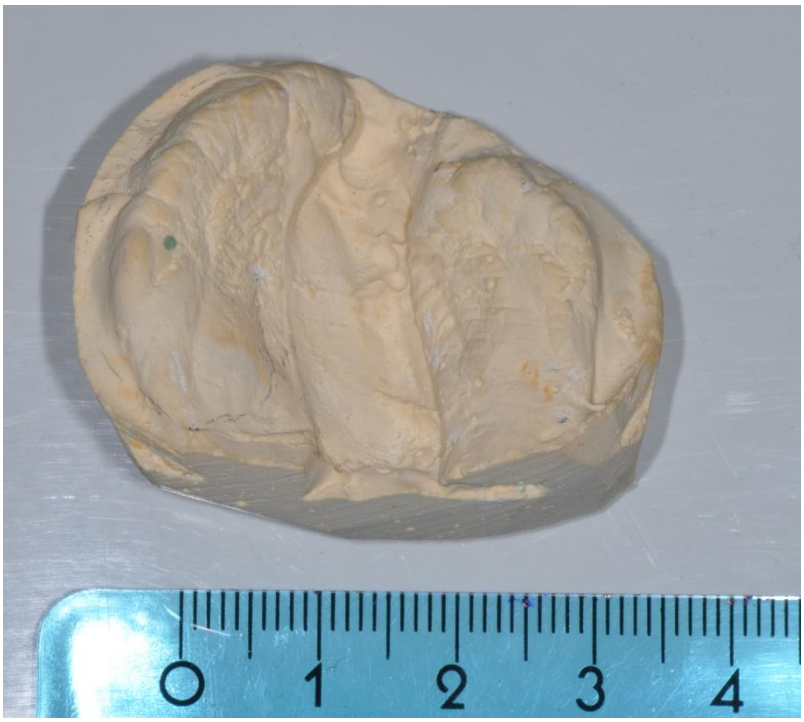

Fig. 38. **Dental cast before presurgical orthopedics.**

Fig 39. **Dental cast after presurgical orthopedics, but before cheiloplasty.**

Fig 40. **Dental cast after cheiloplasty.**

Fig 41. **The Vectra 3D Imaging Stereophotogrammetric System. www.canfieldsci.com Accessed on 14/12/2014.**

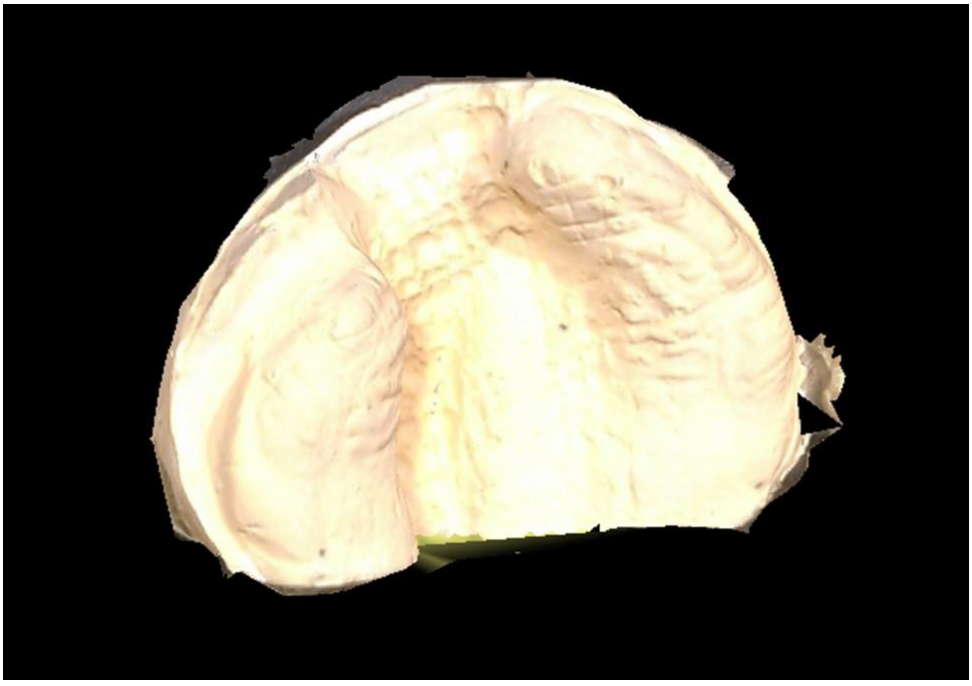

Fig 42. **Digitization of a cast with the stereophotogrammetric system.**

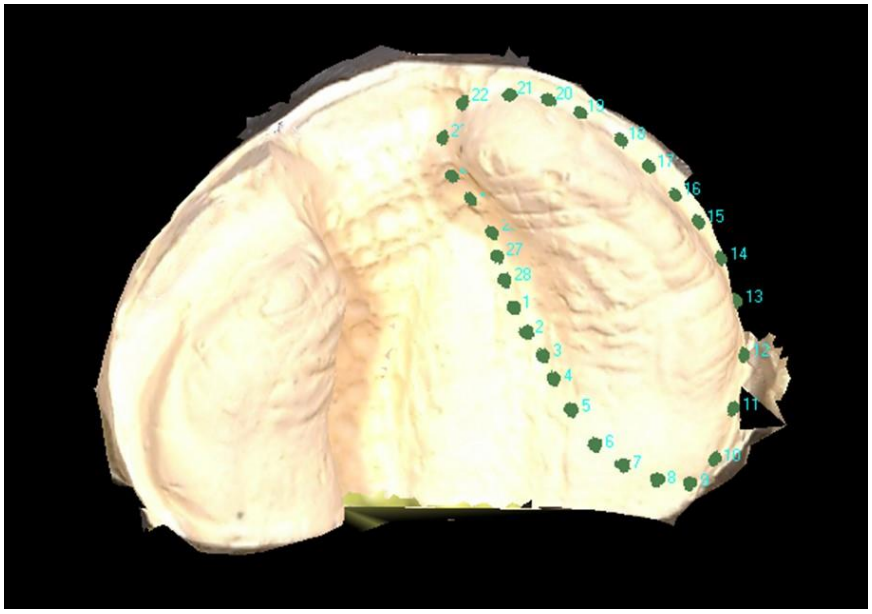

Fig 43. **28 landmarks surround the base of the greater cleft segment, enclosing the area of the alveolar process.**

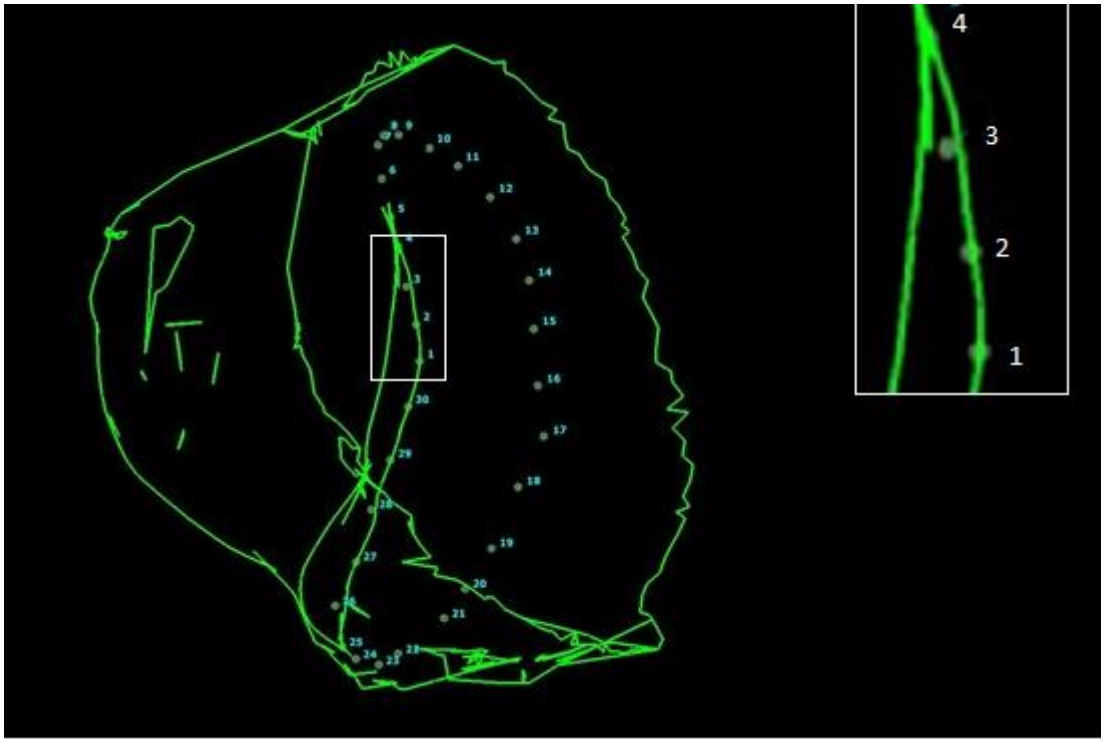

Fig 44. **The tool of the stereophotogrammetric software that shows only the outline of the image (show outline only) can be used to verify that the landmarks (see landmarks 1, 2, 3, 4 in the example) stand on the border (green line).**

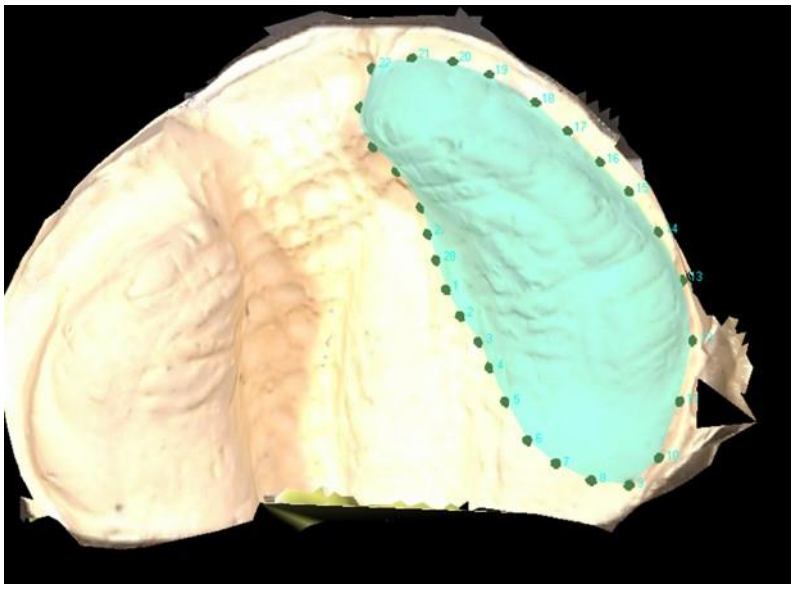

Fig 45. **Area of selection in sky-blue enclosed by the landmarks.**

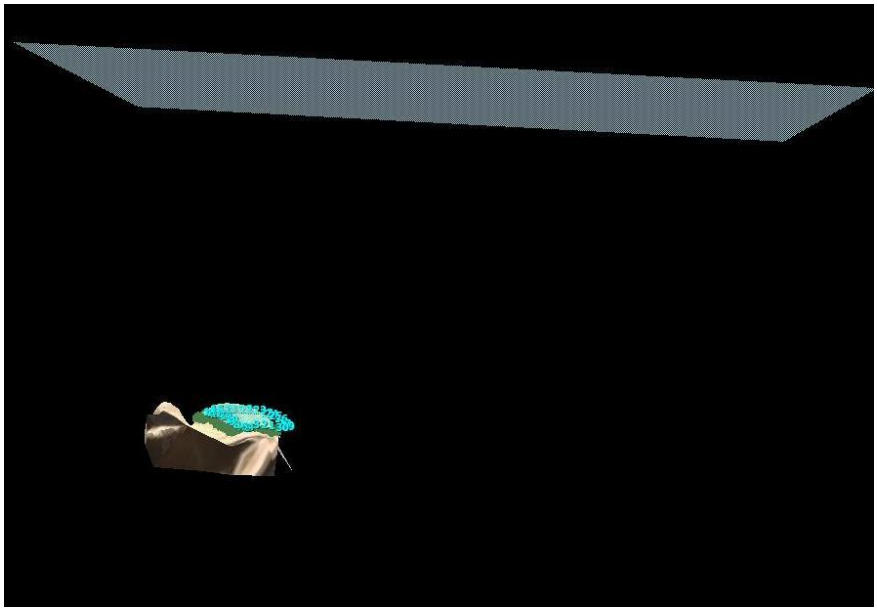

Fig 46. **Importation of a two-dimensional monochromatic plane surface with the dental cast.**

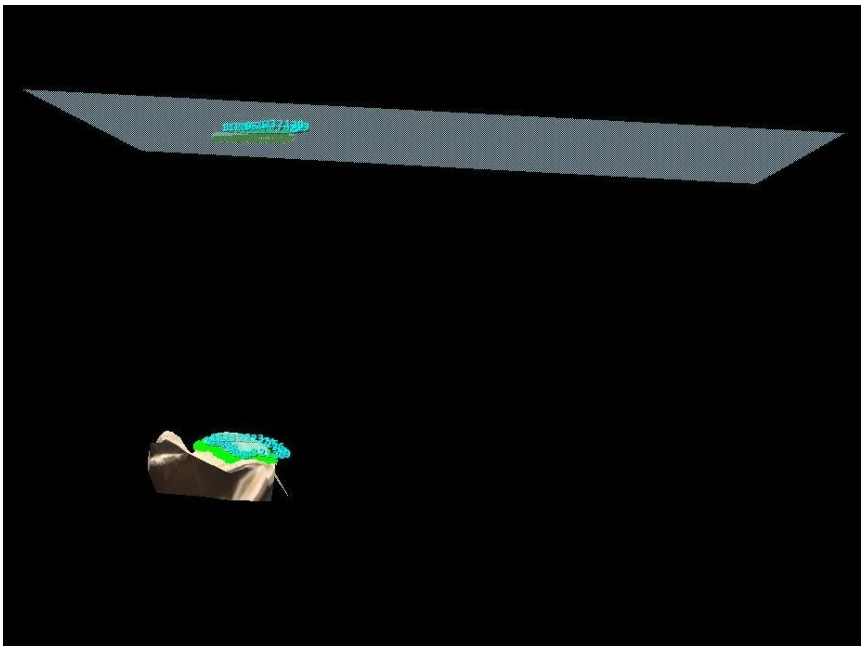

Fig 47. Projection of the landmarks outlining the border of the area on the two-dimensional plane.

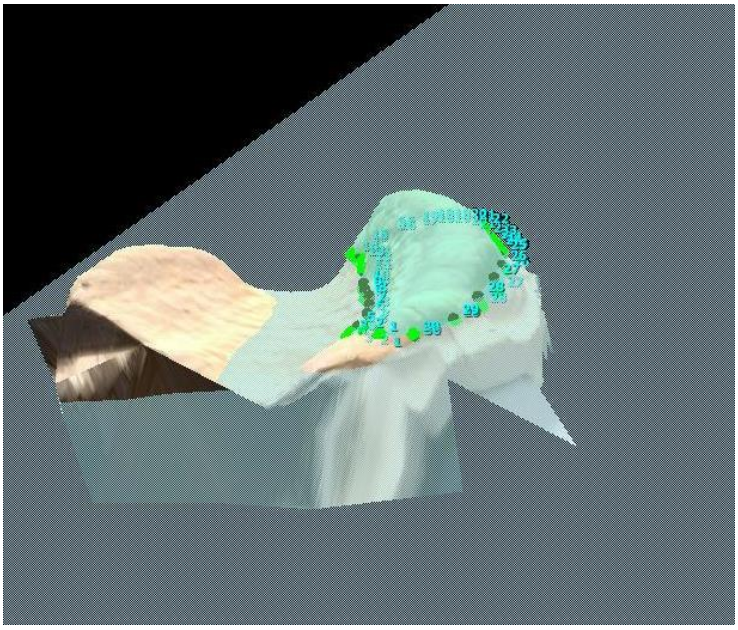

Fig48. The virtual plane cuts the cast at the base of the alveolar process.

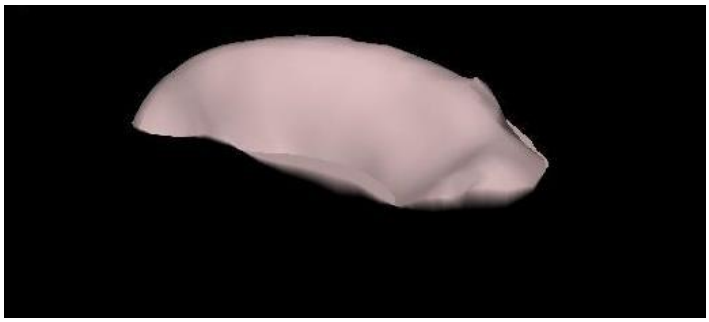

Fig 49. Alveolar process isolated from the cast. Now it is possible to calculate its volume.

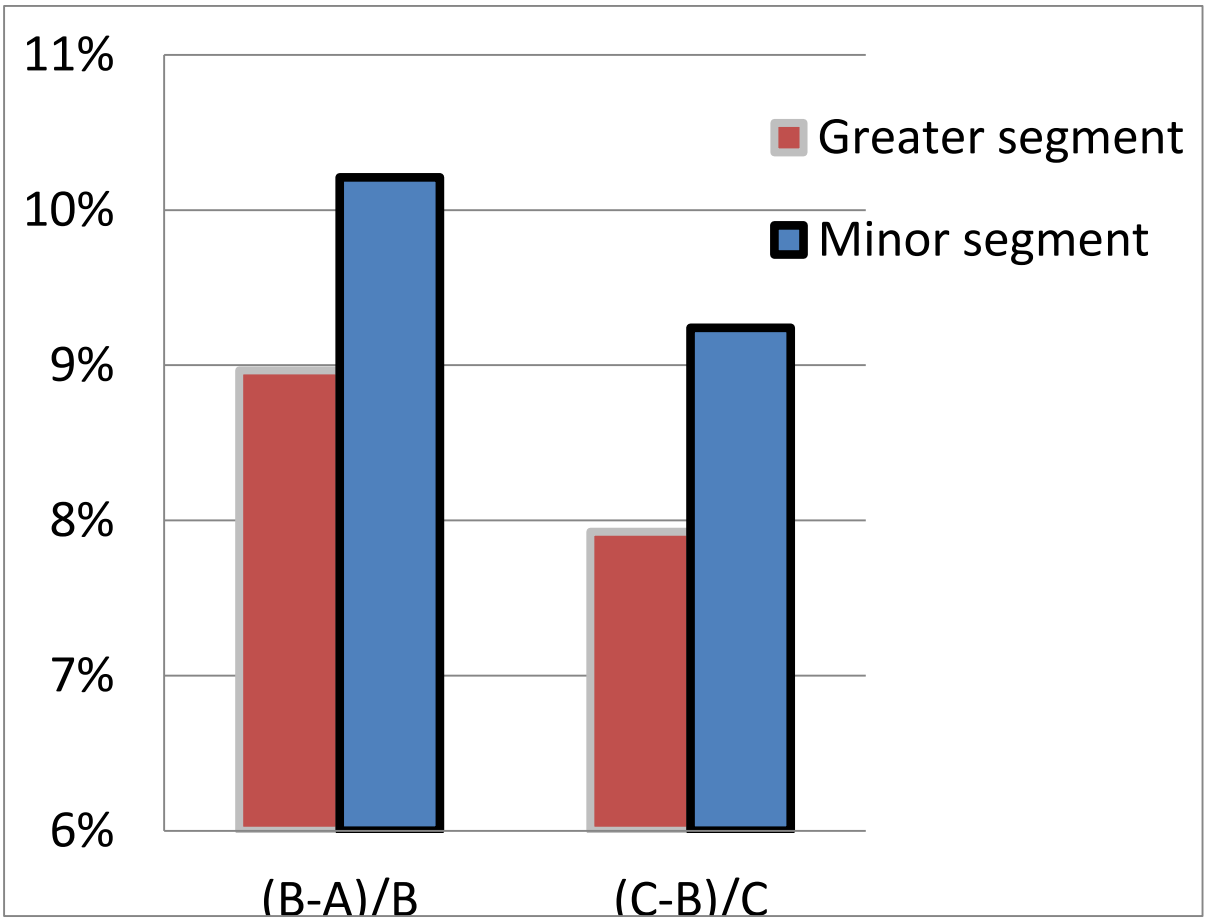

Fig 50. Percentage growth of alveolar area between consecutive time points.

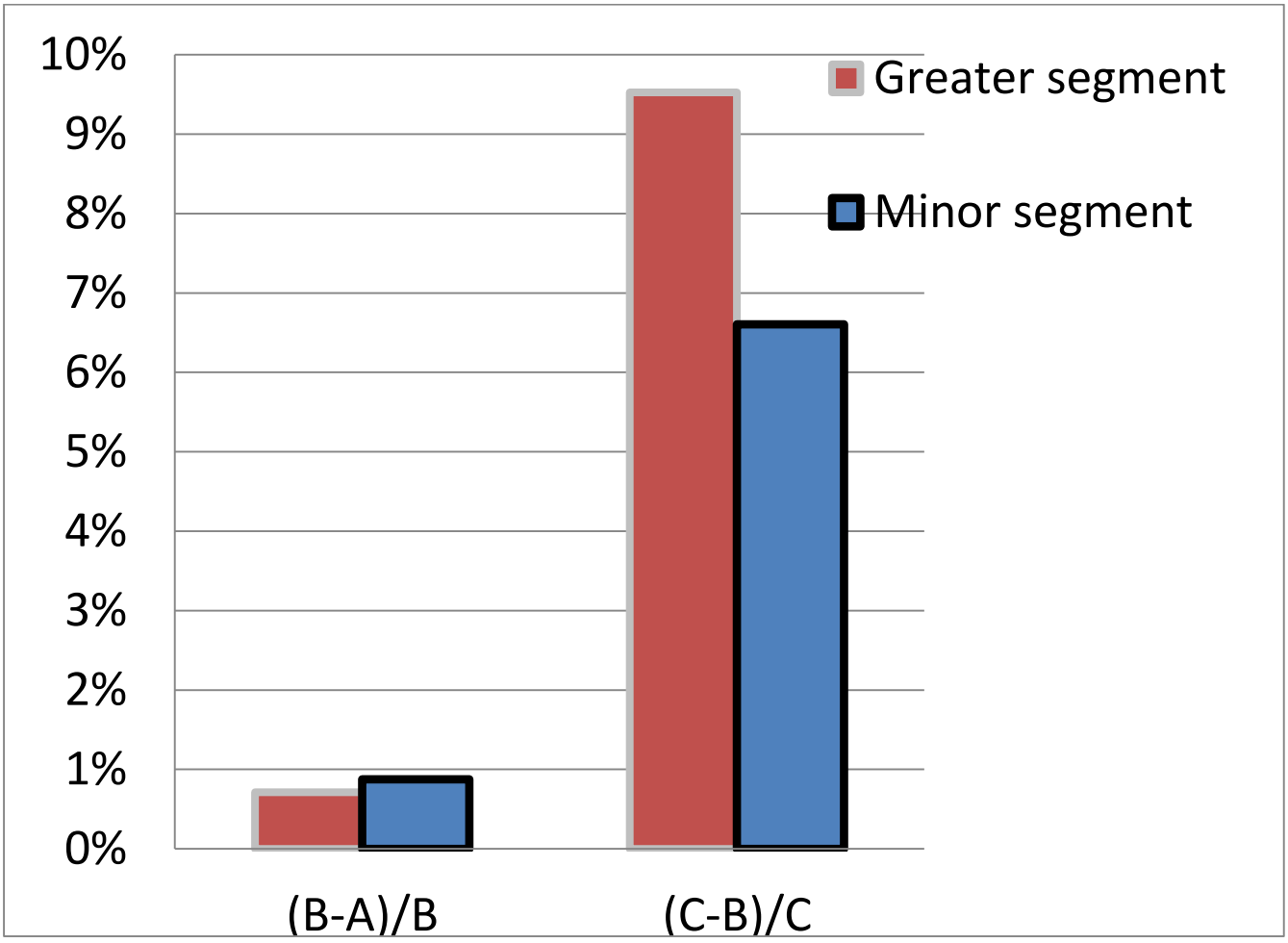

Fig 51. **Percentage growth of alveolar volume between consecutive time points.**

Tables

	O1	O2
1	3.94	3.49
2	4.51	4.65
3	1.79	2.23
4	2.43	2.38
5	3.07	2.99
6	5.56	5.87
7	2.79	3.10
8	4.45	4.31
9	5.15	3.50
10	5.81	6.17
11	4.48	5.28
12	7.41	7.90
13	2.44	2.09
14	3.30	2.97
15	2.91	3.29
16	6.08	6.42
17	3.96	4.27
18	4.02	4.19
19	4.48	4.57
20	5.90	5.89
21	3.70	3.72
22	7.16	7.03
23	2.81	2.45
24	3.60	3.73
25	3.31	2.72
26	5.74	5.59
27	4.53	4.42
28	5.29	4.72
29	6.61	7.15
30	5.55	5.42

	S1	S2
1	3.94	3.94
2	4.51	4.43
3	1.79	1.97
4	2.43	2.57
5	3.07	2.94
6	5.56	5.31
7	2.79	2.68
8	4.45	4.03
9	5.15	4.10
10	5.81	6.16
11	4.48	4.49
12	7.41	7.96
13	2.44	2.39
14	3.30	3.43
15	2.91	2.86
16	6.08	6.24
17	3.96	4.08
18	4.02	4.48
19	4.48	4.57
20	5.90	5.98
21	3.70	4.05
22	7.16	7.41
23	2.81	2.93
24	3.60	3.83
25	3.31	3.24
26	5.74	5.57
27	4.53	4.57
28	5.29	5.12
29	6.61	6.77
30	5.55	5.40

Table 3. Repeatability of the operator's tracings between different operators (O1-O2) and by the same operator over time (S1-S2) on 30 measurements out of the minor or the greater maxillary segment of the casts. All measurements are in cm^2.

Operator		Mean	SD	P value	TEM (cm²)
Inter operator	O1	4.43	1.47	0.92	0.32
	O2	4.42	1.58		
Intra operator	S1	4.43	1.47	0.65	0.21
	S2	4.45	1.51		

Table 4. **Mean, Standard deviation and statistical comparisons of the sample. P-values are from paired Student's t test. TEM: technical error of measurement.**

	Active plate					
	Area					
time	**A**		**B**		**C**	
segment	Min	Gre	Min	Gre	Min	Gre
1	3.94	5.56	4.48	6.08	3.70	5.74
3	1.79	4.45	2.44	4.02	2.81	5.29
5	3.07	5.81	2.91	5.90	3.31	5.55
7	3.99	6.30	3.18	5.43	3.58	4.55
9	2.80	3.97	3.85	6.47	2.71	5.85
11	2.92	5.72	3.29	5.61	5.45	9.31
13	2.82	3.81	3.38	5.63	3.91	5.60
15	3.05	4.53	3.79	5.09	5.17	6.72
17	4.50	8.28	3.81	6.92	3.60	6.76
19	2.35	4.54	3.69	4.93	3.22	5.68
21	4.00	5.56	3.24	6.26	4.60	7.42
23	4.83	6.64	5.16	8.49	5.05	8.02
25	2.07	3.75	1.85	2.16	2.82	5.31
27	3.60	4.60	2.88	6.74	3.70	4.92
29	3.44	5.26	4.12	5.45	4.77	6.63
31	3.70	5.48	3.36	6.55	4.51	8.50

	Passive plate					
	Area					
time	**A**		**B**		**C**	
segment	Min	Gre	Min	Gre	Min	Gre
2	2.79	4.51	3.96	7.41	4.53	7.16
4	2.43	5.15	3.30	4.48	3.60	6.61
6	3.45	5.66	3.92	6.39	5.55	7.73
8	3.06	4.39	3.30	5.88	4.40	6.13
10	3.58	5.59	3.73	4.98	4.33	6.19
12	4.76	8.06	5.26	8.02	5.02	8.70
14	1.98	6.80	2.84	6.43	5.42	8.15
16	2.81	4.55	5.02	8.55	5.28	7.29
18	3.43	6.07	4.51	7.75	4.69	7.53
20	2.74	4.27	3.24	4.25	4.49	5.61
22	3.04	5.69	3.87	8.15	4.11	8.85
24	3.07	4.87	4.35	6.81	4.53	7.20
26	2.83	4.60	3.35	7.56	2.25	7.11
28	2.75	4.53	3.84	5.32	3.64	4.69
30	5.24	5.63	4.10	5.61	4.05	7.59
32	3.69	5.68	3.88	5.76	4.64	5.90

Table 5. **Complete sample of the 32 casts area split by the type of used plate. All values are cm².**

Plate		Time point A		Time point B		Time point C	
		Minor	Greater	Minor	Greater	Minor	Greater
Active	Mean	3.30	5.27	3.46	5.73	3.93	6.37
	SD	0.85	1.18	0.79	1.38	0.89	1.35
Passive	Mean	3.23	5.38	3.90	6.46	4.41	7.03
	SD	0.82	1.01	0.65	1.35	0.81	1.12
Overall	Mean	3.27	5.32	3.68	6.10	4.17	6.70
	SD	0.82	1.09	0.74	1.39	0.87	1.27

Table 6. **Descriptive statistics of area measurements during the follow-up. All values are cm^2.**

	F	P value
Between subject:		
Plate	2.132	0.155
Within subject:		
Time	46.297	<0.0001*
Segment	336.413	<0.0001
Interactions:		
TimeXPlate	2.711	0.110
TimeXSegment	5.161	0.030
TimeXSegmentXPlate	0.041	0.960

Table 7. **Three factor repeated measures analysis of variance. * Pairwise comparison: A vs B, p = 0.001; A vs C, p < 0.001; B vs C, p = 0.003.**

	Active plate					
	Volume					
time	**A**		**B**		**C**	
segment	Min	Gre	Min	Gre	Min	Gre
1	0.80	1.06	1.05	1.14	0.72	1.25
3	0.23	0.74	0.23	0.63	0.38	0.76
5	0.44	1.29	0.43	1.31	0.36	0.97
7	0.80	1.62	0.35	0.86	0.54	0.77
9	0.19	0.50	0.66	1.49	0.27	1.12
11	0.45	1.37	0.38	1.29	1.24	2.66
13	0.36	0.51	0.35	0.97	0.42	0.94
15	0.45	0.79	0.34	0.43	0.76	0.99
17	0.85	2.00	0.50	1.31	0.45	1.51
19	0.25	0.75	0.48	0.59	0.26	0.56
21	0.67	1.28	0.44	1.44	0.87	1.76
23	0.91	1.54	0.97	2.26	1.15	2.01
25	0.31	0.36	0.18	0.29	0.59	0.62
27	0.51	0.70	0.37	0.80	0.92	0.93
29	0.35	1.34	0.69	1.28	0.66	1.47
31	0.87	1.41	0.38	1.41	0.77	1.30

	Passive plate					
	Volume					
time	**A**		**B**		**C**	
segment	Min	Gre	Min	Gre	Min	Gre
2	0.35	0.71	0.73	1.80	0.90	1.46
4	0.38	0.60	0.53	0.80	0.89	1.43
6	0.53	1.23	0.67	1.27	1.21	1.72
8	0.50	0.63	0.60	1.18	0.79	1.27
10	0.60	0.91	0.62	0.78	0.83	1.38
12	1.08	1.59	1.15	0.96	1.09	2.18
14	0.19	1.02	0.27	0.76	0.68	1.21
16	0.69	0.79	0.69	1.22	0.49	1.38
18	0.52	0.54	0.55	0.60	1.00	0.58
20	0.44	0.87	0.51	0.88	0.87	1.11
22	0.42	1.06	0.88	1.96	0.71	2.19
24	0.34	0.78	0.45	0.85	0.58	1.17
26	0.40	0.57	0.63	1.13	0.20	1.30
28	0.46	1.07	0.67	0.80	0.73	1.41
30	0.80	1.32	0.90	1.08	1.03	1.93
32	0.61	0.88	1.08	1.31	1.00	0.45

Table 8. **Complete sample of the 32 casts volume split by the type of used plate. All values are cm^3.**

Plate		Time point A		Time point B		Time point C	
		Minor	Greater	Minor	Greater	Minor	Greater
Active	Mean	0.53	1.08	0.49	1.09	0.65	1.22
	SD	0.25	0.47	0.24	0.49	0.30	0.56
Passive	Mean	0.52	0.91	0.68	1.08	0.81	1.39
	SD	0.21	0.29	0.23	0.37	0.25	0.48
Overall	Mean	0.52	0.99	0.58	1.09	0.73	1.31
	SD	0.23	0.40	0.25	0.43	0.28	0.52

Table 9. **Descriptive statistics of volume measurements during the follow-up. All values are cm^3.**

	F	P value
Between subject:		
Plate	1.19	0.276
Within subject:		
Time	8.58	0.0003*
Segment	96.92	<0.0001
Interactions:		
TimeXPlate	2.05	0.1323
TimeXSegment	0.33	0.721
TimeXSegmentXPlate	0.36	0.7003

Table 10. **Three factor repeated measures analysis of variance. * Pairwise comparison: A vs B, p = 0.096; A vs C, p < 0.001; B vs C, p < 0.001.**

References

Aldridge K., Boyadjiev S.A., Capone G.T., DeLeon V.B., Richtsmeier J.T. Precision and error of three-dimensional phenotypic measures acquired from 3dMD photogrammetric images. Am J Med Genet A 2005;138:247-253.

Altug-Atac A.T., Bolatoglu H., Memikoglu U.T. Facial soft tissue profile following bimaxillary orthognathic surgery. Angle Orthod 2008;78:50-57.

Baek S.H., Son W.S. Difference in alveolar molding effect and growth in the cleft segments: 3 dimensional analysis of unilateral cleft lip and palate patients. Oral Surg Oral Med Oral Pathol Oral Radiol Endod 2006;102:160-168.

Berkowitz S. A multicenter retrospective 3D study of serial complete unilateral cleft lip and palate and complete bilateral cleft lip and palate casts to evaluate treatment: part 1 – the participating institutions and research aims. Cleft Palate Craniofac J 1999;36(5):413-424.

Berkowitz S., Duncan R., Evans C., Friede H., Kuijpers-Jagtman A.M., Prahl-Anderson B., Rosenstein S. Timing of cleft palate closure should be based on the ratio of the area of the cleft to that of the palatal segments and not on age alone. Plast Reconstr Surg 2005;115:1483-1499.

Braumann B., Keilig L., Bourauel C., Niederhagen B., Jager A. 3-dimensional analysis of cleft palate casts. Ann Anat 1999;181:98-98.

Bugaighis I., Mattick C.R., Tiddeman B., Hobson R. 3D facial morphometry in children with oral clefts. Cleft Palate Craniofac J 2014;51(4):452-461.

Burris B.G., Harris E.F. Identification of race and sex from palate dimensions. J Forensic Sci 1998;43:959-963.

Byers S.N. Churchill S.E., Curran B. Identification of Euro-Americans, Afro-Americans, and Amerindians frompalatal dimensions. J Forensic Sci 1997;42(1):3-9.

Ciusa V., Dimaggio F.R., Sforza C., Ferrario V.F. Three-dimensional palatal development between 3 and 6 years. Angle Orthod 2007;77(4):602-606.

Colombo A., Dellavia C., Tartaglia G.M., Ciusa V., Ferrario V.F. Studio tridimensionale della morfologia del palato duro. Mondo Ortodontico 2001;4:245-252.

Corbo M., Dujardin T., de Maertelaer V., Malevez C., Glineur R. Dentocraniofacial morphology of 21 patients with unilateral cleft lip and palate: a cephalometric study. Cleft Palate Craniofac J 2005;42:618-624.

De Ladeira P.R.S., Alonso N. Protocols in cleft lip and palate treatment: systematic review. Plast Surg Int 2012; doi: 10.1155/2012/562892.

Dellavia C., Sforza C., Malerba A., Strohmenger L., Ferrario V.F. Palatal size and shape in 6-year olds affected by hypohidrotic ectodermal dysplasia. Angle Orthod 2006;76(6):978-983.

Dellavia C., Sforza C., Orlando F., Ottolina P., Pregliasco F., Ferrario V.F. Three-dimensional hard tissue palatal size and shape in Down syndrome subjects. Eur J Orthod 2007;29:417-422.

De Menezes M., Rosati R., Ferrario V.F., Sforza C. Accuracy and reproducibility of a 3-dimensional stereophotogrammetric imaging system. J Oral Maxillofac Surg 2010;68:2129-2135.

Demke J.C., Tatum S.A. Analysis and evolution of rotation principles in unilateral cleft lip repair. J Plast, Reconstr Aesthet Surg 2011;64:313-318.

Eichhorn W., Blessmann M., Vorwig O., Gehrke G., Schmelzle R., Heiland M. Influence of lip closure on alveolar cleft width in patients with cleft lip and palate. Head Face Med 2011;7:3.

Ferrario V.F., Sforza C., Miani A. jr., Tartaglia G. Mathematical definition of the shape of dental arches in human permanent healthy dentitions. Eur J Orthod 1994;16:287-294.

Ferrario V.F., Sforza C., Miani A. jr. Statistical evaluation of Monson's sphere in healthy permanent dentitions in man. Archs Oral Biol 1997;42(5):365-369.

Ferrario V.F., Sforza C., Schmitz J.H., Colombo A. Quantitative description of the morphology of the human palate by a mathematical equation. Cleft Palate Craniofac J 1998;35(5):396-401.

Ferrario V.F., Sforza C., Colombo A., Tartaglia G.M. The effect of ethnicity and age on palatal size and shape: a study in a northern Chilean healthy population. Int J Adult Orthod Orthognath Surg 2000;15(3):233-240.

Ferrario V.F., Sforza C., Colombo A., Dellavia C., Dimaggio F.R. Three-dimensional hard tissue palatal size and shape in human adolescents and adults. Clin Orthod Res 2001;4:141-147.

Ferrario V.F., Sforza C., Dellavia C., Colombo A., Ferrari R.P. Three-dimensional hard tissue palatal size and shape: a 10-year longitudinal evaluation in healthy adults. Int J Adult Orthod Orthognath Surg 2002;17(1):51-58.

Ferrario V.F., Sforza C., Dellavia C., Tartaglia G.M. Sozzi D., Carù A. A quantitative three-dimensional assessment of abnormal variations in facial soft tissues of adult patients with cleft lip and palate. Cleft Palate Craniofac J 2003;40(5):544-549.

Gandolfini M., Melegari M., Mannucci N., Sesenna E., Bonanini M., Gennari P.U. Il trattamento ortodontico-ortopedico delle labiopalatoschisi e loro esiti. Masson 1993;15-36.

Gesch D., Kirbschus A., Mack F., Gedrange T. Comparison of craniofacial morphology in patients with unilateral cleft lip, alveolus and palate with and without secondary osteoplasty. J Cranio Maxillofac Surg 2006;34:62-66.

Grabowski R., Kopp H., Stahl F., Gundlach K.K. Presurgical orthopaedic treatment of newborns with clefts-functional treatment with long-term effects. J Craniomaxillofac Surg 2006;34(2):34-44.

Gray H. Anatomy of the Human Body. Philadelphia: Lea & Febiger, 1918. Published May 2000 by Bartleby.com; Available at www.bartleby.com/107/.

Heidbuchel K.L., Kuijpers-Jagtman A.M., Van't Hof M.A., Kramer G.J., Prahl-Andersen B. Effects of early treatment on maxillary arch development in BCLP. A study on dental casts between 0 and 4 years of age. J Craniomaxillofac Surg 1998;26:140-147.

Heike C.L., Cunningham M.L., Hing A.V., Stuhaug E., Starr J.R. Picture perfect? Reliability of craniofacial anthropometry using three-dimensional digital stereophotogrammetry. Plast Reconstr Surg 2009;124:1261-1272.

Ishida F., Mashiko M., Shimabukuro I., Yamamoto S., Shimizu K., Maeda T. 3-D image analysis on palate growth changes from birth to 1 month in healthy infants. Ped Dent J 2013;23:37-43.

Johnson J.M., Moonis G., Green G.E., Carmody R., Burbank H.N. Syndromes of the first and second branchial arches, part 1: embryology and characteristic defects. Am J Neuroradiol 2011;32:14-19.

Kasaven C.P., Ivekovic S., Mcintyre G.T., Gillgrass T., Thomson D.A., Menhinick A., Mossey P.A. Validation of the volumetric measurements of a simulated maxillary alveolar bone defect using cone-beam computed tomography. Cleft Palate Craniofac J 2013;50(6):115-120.

Ladner P.T., Muhl Z.F. Changes concurrent with orthodontic treatment when maxillary expansion is a primary goal. Am J Orthod Dentofacial Orthop 1995;108:184-193.

Lopez-Palacio A.M., Ceron-Zapata A.M., Gomez D.F., Davila-Calle A.P., Ojalvo-Arias M.A. Nasal changes with nasoalveolar molding in colombian patients with unilateral cleft lip and palate. Ped Dent 2012;34:239-244.

Mello B.Z., Fernandes V.M., Carrara C.F., Machado M.A., Garib D.G., Oliveira T.M. Evaluation of the intercanine distance in newborns with cleft lip and palate using 3D digital casts. J Appl Oral Sci 2013;21:437-442.

Miller S.F., Weinberg S.M., Nidey N.L., Defay D.K., Marazita M.L., Wehby G.L., Moreno Uribe L.M. Exploratory genotype-phenotype correlations of facial form and asymmetry in unaffected relatives of children with non-syndromic cleft lip and/or palate. J Anat 2014; doi: 10.1111/joa.12182.

Moore K.L. Before we are born: basic embryology and birth defects. 3rd edition. Philadelphia: W.B. Saunders; 1989;134-158.

Mossey P. Epidemiology underpinning research in the aetiology of orofacial clefts. Orthod Craniofac Res 2007;10:114-120.

Mossey P.A., Little J., Munger R.G., Dixon M.J., Shaw W.C. Cleft lip and palate. Lancet 2009;1773-1785.

Mosmuller D.G.M., Don Griot J.P.W., Bijnen C.L., Niessen F.B. Scoring systems of cleft-related facial deformities: a review of literature. Cleft Palate Craniofac J 2013;50(3):286-296.

Muchitsch A.P., Winsauer H., Wendl B., Pichelmayer M., Kuljuh E., Szalay A., Muchitsch M. Remodelling of the palatal dome following rapid maxillary expansion (RME): laser scan-quantifications during a low growth period. Orthod Craniofac Res 2012;15:30-38.

Naidu D., Scott J., Ong D., Ho C.T. Validity, reliability and reproducibility of three methods used to measure tooth widths for Bolton analyses. Aust Orthod J 2009;25:97-103.

Otero L., Bermudez L., Lizarraga K., Tangco I., Gannaban R., Meles D. A comparative study of facial asymmetry in Philippine, Colombian, and Ethiopian families with nonsyndromic cleft lip palate. Plast Surg Int 2012;580769.

Papadopoulos M.A., Koumpridou E.N., Vakalis M.L., Papageorgiou S.N. Effectiveness of pre-surgical infant orthopedic treatment for cleft lip and palate patients: a systematic review and meta-analisys. Orthod Craniofac Res 2012;15:207-236.

Papamanou D.A., Gkantidis N., Topouzelis N., Christou P. Appreciation of cleft lip and palate treatment outcome by professionals and laypeople. Eur J Orthod 2012;34(5):553-560.

Penna V., Stark G.B., Eisenhardt S.U., Bannasch H., Iblher N. The aging lip: a comparative histological analysis of age-related changes in the upper lip complex. Plast Reconstr Surg 2009;124(2):624-628.

Prahl C., Kuijpers-Jagtman A., van't Hof M.A., Prahl-Andersen B. A randomized prospective clinical trial into the effect of infant orthopaedics on maxillary arch dimensions in unilateral cleft lip and palate (Dutchcleft). Eur J Oral Sci 2001;109:297-305.

Proff P., Weingartner J., Rottner K., Bayerlein T., Schoebel S., Kaduk W., Gedrange T. Functional 3D analysis of patients with unilateral cleft of lip, alveolus and palate (UCLAP) following lip repair. J Craniomaxillofac Surg 2006;34(2):26-30.

Restrepo C.C., Sforza C., Colombo A., Pelaez-Vargas A., Ferrario V.F. Palate morphology of bruxist children with mixed dentition. A pilot study. J Oral Rehab 2008;35:353-360.

Rousseau P., Metzger M., Frucht S., Schupp W., Hempel M., Otten J.E. Effect of lip closure on early maxillary growth in patients with cleft lip and palate. Facial Plast Surg 2013;15:369-373.

Russell K.A., Tompson B., Paedo D. Correlation between facial morphology and esthetics in patients with repaired complete unilateral cleft lip and palate. Cleft Palate Craniofac J 2009;46:319-325.

Sabarinath V.P., Thombare P., Hazarey P.V., Radhakrishnan V., Agrekar S. Changes in maxillary alveolar morphology with nasoalveolar molding. J Clin Ped Dent 2010;35:207-212.

Sforza C., de Menezes M., Bresciani E., Ceron-Zapata A.M., Lopez-Palacio A.M., Rodriguez-Ardila M.J., Berrio-Gutierrez L.M. Evaluation of a 3D Stereophotogrammetric technique to measure the stone casts of patients with unilateral cleft lip and palate. Cleft Palate Craniofac J 2012;49(4):477-483.

Sforza C., de Menezes M., Ferrario V.F. Soft- and hard-tissue facial anthropometry in three dimensions: what's new. J Anthropol Sci 2013;91:159-184.

Simanka E., Morris D., Zhao L., Reisberg D., Viana G. Measuring progressive soft tissue change with nasoalveolar molding using a three-dimensional system. J Craniofac Surg 2011;22:1622-1625.

Tse R., Booth L., Keys K., Saltzman B., Stuhaug E., Kapadia H., Heike C. Reliability of nasolabial anthropometric measures using three-dimensional stereophotogrammetry in infants with unrepaired unilateral cleft lip. Plast Reconstr Surg 2014;133(4):530e-542e.

Weinberg S.M., Scott N.M., Neiswanger K., Brandon C.A., Marazita M.L. Digital three-dimensional photogrammetry: evaluation of anthropometric precision and accuracy using a Genex 3D camera system. Cleft Palate Craniofac J 2004;41:507-518.

Weinberg S.M., Naidoo S., Govier D.P., Martin R.A., Kane A.A., Marazita M.L. Anthropometric precision and accuracy of digital three-dimensional photogrammetry: comparing the Genex and 3dMD imaging systems with one another and with direct anthropometry. J Craniofacial Surg 2006;17:477-483.

Williams P., Warwick R., Dyson M., Bannister L.H. Gray's anatomy. Thirty-seventh edition. Churchill livingstone, 1989.

Wong J.Y., Oh A.K., Ohta E., Hunt A.T., Rogers G.F., Mulliken J.B., Deutsch C.K. Validity and reliability of craniofacial anthropometric measurement of 3D digital photogrammetric images. Cleft palate craniofac J 2008;45:232-239.

Yamada T., Mori Y., Mishima K., Sugahara T. Nasolabial and alveolar morphology following presurgical orthopaedic treatment in complete unilateral clefts of lip, alveolus and palate. J of Cranio-maxillofac Surg 2003;31:343-347.

Yamanishi T., Nishio J., Kohara H., Hirano Y., Sako M., Yamanishi Y., Adachi T., Miya S., Mukai T. Effect on maxillary arch development of early 2-stage palatoplasty by modified Furlow technique and conventional 1-stage palatoplasty in children with complete unilateral cleft lip and palate. J Oral Maxillofac Surg 2009;67(10):2210-2216.

Young G. Cleft lip and Palate. Available at http://www2.utmb.edu/otoref/Grnds/Cleft-lip-palate-9801.htm. Accessed on 14/12/2014.

Zayed E.F., Ayad W., Moustafa W.A., Abdul-Hameed M., El-Shishtawy M. Unilateral cleft lip repair: experience with Millard technique and introduction to the concept of junctional zones repair. J Plast Reconstr Surg 2012;36(2):109-118.

http://nursingcrib.com/. Accessed on 14/12/2014.

http://www.eurocran.org/. Accessed on 14/12/2014.